TR-138
1985

Improving Surge Flow Irrigation Efficiency Based on Analysis of Infiltration and Hydrodynamic Effects

E.T. Smerdon
A.W. Blair

Texas Water Resources Institute

Texas A&M University

RESEARCH PROJECT COMPLETION REPORT

Project Numbers
G-871-04
G-935-05
(July 1, 1983 - July 31, 1984)
(July 17, 1984 - July 31, 1985)

Agreement Numbers
14-08-0001-G-871
14-08-0001-G-935

IMPROVING SURGE FLOW IRRIGATION EFFICIENCY BASED ON ANALYSIS OF INFILTRATION AND HYDRODYNAMIC EFFECTS

by

Ernest T. Smerdon
Allie W. Blair

Submitted to

Geological Survey
U.S. Department of the Interior
Reston, Virginia 22092

The research on which this report is based was financed in part by the U.S. Department of the Interior, Geological Survey, through the Texas Water Resources Institute.

Technical Report No. 138
Texas Water Resources Institute
Texas A&M University
College Station, Texas 77840-2118

July 1985

Table of Contents

List of Figures

List of Tables

IMPROVEMENT OF SURFACE IRRIGATION EFFICIENCY USING SURGE FLOW INFILTRATION AND HYDRODYNAMIC EFFECTS

A. ABSTRACT

This research investigated the movement of a surface flow profile over an infiltrating soil under conditions of surge flow, and theory related thereto, for use in preliminary design procedures for surge irrigation systems. Four specific research areas were: a) development of a surge flow infiltration model; b) the effect of wetted perimeter on infiltration in furrow; c) design, construction, and calibration of a physical model of an irrigation border/furrow; and d) development of a surge flow furrow irrigation computer model for use in designing surge flow irrigation systems.

The effect of wetted perimeter on infiltration in furrows was investigated using field data. Overall, the Kostiakov cumulative infiltration equation, modified to include wetted perimeter raised to a power greater than unity, appeared to satisfactorily represent the effect of wetted perimeter on infiltration in furrows.

The effect of surge flow cycle time and cycle ratio on infiltration in furrows was investigated using a recirculating furrow infiltrometer which simulates surge flow irrigation for various cycle times and cycle ratios. The data collected were used to evaluate two empirical surge flow infiltration models. The effects of furrow geometry, surface storage, and recession time were considered. The results indicated that infiltration during surge flow irrigation can be effectively described using an empirical model based on the Kostiakov cumulative infiltration equation, the surge cycle ratio, and the surge cycle time.

A physical model of an irrigation border/furrow was constructed using a 61 meter long by 0.76 meter wide tilting flume with a 0.09 meter deep infiltrating gravel bed. The model was partitioned into 15 sections of equal length. Each section contained a small computer controlled submersible pump by which water was uniformly withdrawn from the section through the gravel bed. Real time predictor/corrector computer algorithms were developed to simulate discrete spatially and temporally varying nonlinear infiltration. Each partitioned section also contained an electronic water depth sensor. All 15 water depth sensors are connected to a real time data acquisition system which relays depth of flow information to the computer simulating infiltration. The hydraulic effects of the infiltration simulator partitions, the effect of downstream boundaries on upstream flow depths, and the effect of flow depth and velocity distribution on energy loss were investigated.

A computer model of surge flow hydraulics and infiltration was developed for the preliminary design of surge flow systems. The model is based on the

kinematic wave assumptions for overland flow, and the cycle ratio-time infiltration model developed during this research project. Hypothetical irrigation simulations indicate that for some high intake rate soils, surge flow has potential for markedly improving distribution efficiency over conventional continuous irrigation. However, the model also indicated that an improperly operated surge flow system can actually have lower efficiency than a continuous flow system; this factor is seldom mentioned in literature on surge irrigation.

B. PURPOSE OF RESEARCH AND INTRODUCTION

How to meet future water demands with a decreasing supply is a critical problem in Texas. Water conservation must play an important role. This research focuses on improving the water use efficiency of irrigation by developing procedures for designing surge irrigation systems. This research is extremely important in the High Plains area of Texas, where the water supply to support irrigation is declining. Surge flow irrigation is one of three potentially highly efficient irrigation methods. The other two, drip and low energy precision application sprinklers, cost several times as much per acre of irrigated crop. The potential water savings from surge irrigation in Texas is between 1 and 2 million acre feet per year. This magnitude is illustrated by comparing it with the 3 million acre feet per year of domestic water use in Texas.

This research is directed at the problem of water conservation in irrigated agriculture; it is particularly applicable to irrigation in the the High Plains region of Texas. In 1982, Texas High Plains farmers produced $1.6 billion in crops--about 40% of the total Texas farm crop income. To further illustrate the importance of High Plains irrigation, this crop income generates another $3.5 billion in economic activity in supplies and services for a total economic contribution to the state in excess of $5.0 billion in 1982. However, the water level in the Ogallala aquifer which supplies the irrigation is declining and less water is available each year to support irrigation. It is imperative that everything possible be done to extend the High Plains groundwater supply.

Most of the irrigation in the High Plains is by the surface irrigation method. Moreover, surface irrigation accounts for over 60% of all irrigated crop land in the United States (Irrigation Journal 1985) and a much higher percentage over the world. Unfortunately, surface irrigation is often quite inefficient with less than half the water applied ending up in the crop root zone where it is available to be used by the crop.

Definition of Surge Flow. Surge flow irrigation is an overland flow process with a cyclic inflow hydrograph, and is applicable to most types of surface irrigation systems. Surge irrigation is characterized by a period of flow followed by a period without flow. Two basic terms used to desribe the ON-OFF periods are cycle ratio and cycle time. The cycle time, t_c, is the total time to complete one cycle, including both on and off periods. The cycle ratio, r, is the fraction of time water is delivered during the cycle time. An example cycle time of 1 hour and a cycle ratio of 0.25 would produce an inflow hydrograph with a period of flow for 15 minutes followed by a period without flow for 45 minutes.

Commercial surge flow systems are limited to gated pipe systems primarily because these systems are easy to automate, and are used on many farms. Most gated pipe systems are used for furrow irrigation. Since commericial surge flow systems use pillow or butterfly valves, it is convenient to view the cyclic inflow hydrograph as the result of a valve sequencing pattern (VSP). This pattern consists of a sequence of valve ON-OFF periods with each cycle defined by a cycle ratio and time. The cycle ratio and time are not necessarily constant for every cycle, although constant values are used in most commercial systems.

Surge irrigation has been shown to markedly improve the efficiency of water application under some circumstances (Blair 1984). However, the reasons for the improvement have not been sufficiently well understood to permit irrigation engineers to predict how effective surge irrigation will be under different soils and local conditions. In fact, it has not been possible to scientifically design a surge irrigation system which will optimize the water application efficiency, considering the many irrigation variables involved. Some important surge irrigation design and operation variables include cycle time and cycle ratio. These should be considered along with all the other variables in surface irrigation design including soil properties, stream size, length of run, and furrow slope, to name some of the more important factors.

Surge irrigation performance has to be explained by analysis of the physical processes involved. These include: (a) changes in the "effective" soil infiltration which results from the surge process and (b) overland flow hydrodynamics as changed by the cyclic water flow to the furrows. This research was directed toward finding the physical and mathematical explanation for the improvement of the irrigation efficiency by surge irrigation. The results of these findings were used to develop a preliminary design procedure for surge flow furrow irrigation systems.

C. OBJECTIVES

The objective was to investigate the movement of a surface flow profile over an infiltrating soil under conditions of surge flow and to develop and verify theory related thereto for use in design procedures for surge irrigation systems. Four specific objectives were:

a) Investigate the effect of wetted perimeter and furrow geometry on infiltration and develop an empirical infiltration model to describe these effects.

b) Investigate the effect of surge flow cycle ratio and cycle time on infiltration in furrows, and develop an empirical model to describe these effects.

c) Design, build, and calibrate a physical model of an irrigation border/furrow. The model will be used in a continuing USGS funded research project to investigate the complex hydraulic relationships involved in surge flow.

d) Develop a computer model for use in preliminary design of surge irrigation systems.

D. RELATED PREVIOUS AND ONGOING RESEARCH

D.1 Previous Research

Previous research involves four major areas: surge flow advance studies, surge flow infiltration studies, physical hydraulic modeling, and design methods. Because of the differences between these areas, research pertaining to each will be outlined separately. Note that this section outlines the results of published research including four publications which have resulted from this project (Blair and Smerdon 1985a, Blair and Smerdon 1985b, Blair and Smerdon 1985c, Blair, Smerdon and Rutledge 1984).

Surge Flow Advance Studies. Walker, Henggler, and Bishop (1981) measured the effects of surge flow in level basins. They concluded that surge flow increased uniformity of the distribution of water and reduced infiltration rates. Also, they stated that additional research is needed before any major conclusions are to be made. Walker and Lee (1981) evaluated the kinematic wave computer model for surge and continuous inflow in furrows. They concluded that specific numerical methods should be used and that the limitations of their models have not been completely researched. Bishop, Walker, Allen, and Poole (1981) evaluated surge flow advance in a 600-foot long silt loam furrow. They indicated that surge flow advanced water quicker than continuous flow and they postulated that the phenomenon responsible for the quickened advance was reduced infiltration.

Coolidge, Walker, and Bishop (1982), evaluated various cycle times for surge flow using field data from 300-foot long furrow sections in a field with a silt loam soil. The results indicated that surge flow advances water quicker than continuous flow and reduces variability in advance rates between furrows. Elliott, Walker, Skogerboe (1982) evaluated the zero-inertia form of the Saint Venant equations using field data obtained during continuous flow furrow irrigation. The modified Kostiakov equation was used to describe infiltration characteristics. The results indicated that the zero-inertia method was accurate in predicting advance, provided the infiltration characteristics were accurately defined.

Podmore and Duke (1982) evaluated surge flow irrigation system hardware and field tests. They found that their hardware system performed adequately. Also, reduction in infiltration rates and increased efficiencies were noted. They suggested that more research was needed to determine the physical processes associated with surge flow and the methods used to manage surge flow. Walker and Bishop (1982) evaluated surge flow using field tests. They concluded that for sandy soils, surge flow could accomplish the advance phase of irrigation with half the water required for continuous flow. Walker and Humphreys (1983) evaluated the kinematic wave model for both continuous and surge flow furrow irrigation using field data from several sites. These authors concluded that the kinematic wave model is accurate in predicting advance for both surge and continuous flow, given

the infiltration characteristics are adequately described, and the irrigated field is free draining and sloping.

Izuno and Podmore (1984) developed a kinematic wave model for surge irrigation based on Walker and Humphrey's (1983) work. They reported that the accuracy with which roughness, furrow shape, and bed slope are measured has little effect on the kinematic wave model efficiency predictions. However, Strelkoff and Souza (1985) reported that roughness and furrow shape can be critical in determining efficiencies because of their influence on wetted perimeter in the furrow, and the large effect that wetted perimeter has on infiltration. Blair and Smerdon (1985a) also reported that wetted perimeter has a significant influence on infiltration in furrows. These results were from studies under this project.

Surge Flow Infiltration Studies. Zur (1976) proposed a pulsed drip irrigation method and evaluated the method using vertical soil columns. He applied a point source of water for different rates and durations, and measured soil water content vs. depth and advance rate of the wetting front. The application rate was such that ponding of water was not allowed. He concluded that water content at equilibrium decreased as the time-averaged application rate decreased, and the time-averaged advance rate of the wetting front for pulsed application was similar to the advance rate for continuous application.

Malano (1983) used field data obtained with a recirculating furrow infiltrometer to investigate surge flow infiltration. He concluded that surge flow infiltration rate was significantly less than continuous flow infiltration rate. Samani (1983) performed a comprehensive investigation of possible mechanisms involved in surge flow infiltration. He performed field, laboratory, and computer simulation of surge flow infiltration using a two dimensional Richard's equation model. He concluded that soil consolidation and sedimentation have important roles in reducing infiltration rates. Blair, Smerdon, and Rutledge (1984), based on work in the early phases of this project, proposed a cycle ratio-time surge flow infiltration model based on a continuous flow infiltration equation and the characteristics of surge flow. Izuno, Podmore, and Duke (1984) suggested a step function surge flow model which assumes that infiltration rate becomes constant after the initial surge. In more work under this project, Blair and Smerdon (1985b) evaluated the cycle ratio-time model and the step function model using infiltrometer data for various cycle ratios and cycle times. They concluded that the cycle ratio-time model was slightly more accurate than the step function model.

Physical Hydraulic Modeling. Wessels and Strelkoff (1968) studied the effect of roughness on water surface profiles in a 32 ft rectangular tilting flume with an impervious bed. They recommended that a longer flume be used to better simulate flow profiles which are likely to exist in typical irrigated borders. Jobling and Turner (1973) studied the effect of infiltration on water surface profiles using a 60 ft rectangular flume. Infiltration was simulated by using cylindrical containers connected to the center of each sqaure foot of the flume. The initial infiltration rate was controlled by the number of openings connecting each cylinder to the flume, and the constant rate was controlled by the size of the outlet orifice in the bottom of the cylinder. They concluded that depth of flow during the advance of

water down the flume could be described as an empirical power function of the advance distance times the flow depth at the inlet of the flume. They also noted that the large amount of labor required to perform each experiment limited their investigation into the effects of various infiltration rates, slopes and inflow rates. No known surge flow research, except for that performed by the authors of this report and described herein, has been performed using a flume.

Design Methods. Many articles and several monographs have been written about design procedures for border and furrow irrigation systems. The SCS (1974) and ASAE (1980) have published two of these monographs. Both of these monograph use the concepts of irrigation distribution and application efficiency in their design procedures. Smerdon and Glass (1964) outlined a procedure using dimensionless variables to determined the ratio of the time required for the wetting front to advance to the end of the furrow to the time required for the average depth of water to infiltrate. Strelkoff and Shatanawi (1985) used normalized dimensionless graphs prepared using the zero inertia model to determine distribution and application efficiencies. The addition complexity of surge flow limits the applicability of these type of design methods. Alternatively, a computer model of surge flow was developed (under this project) which, through a trial and error approach, can be used to evaluate and design a surge flow irrigation system. After additional research and development this computer model will be available for use on a personal computer (IBM-PC) for use by practicing engineers. The specifics of the proposed design procedures are outline in the **Methodology** section of this report.

D.2 Ongoing Research

Currently the USDA ARS sponsored Western Regional Research Project (W-163) concerns surge flow irrigation. The investigators on this project are working with researchers in other states participating in W-163. Currently research data collection and terminology are being standardized, research objectives defined, and research results disseminated. The project involves researchers from California, Colorado, Utah, Washington, New Mexico, and Texas. The Ph.D. candidate for this proposal, Al Blair, has participated in three meetings of Project W-163 and arranged for an exchange of data with investigators in several western states doing field work in surge irrigation. Mr. Blair is currently the chairman of the sub-committee on Standardization and Design of the Recirculating Furrow Infiltrometer. Mr. Blair is also cooperating with the SCS, ARS, and High Plains Underground Water Conservation District No. 1 in field work on surge irrigation in Texas and has presented a seminar on this work to the High Plains Underground Water Conservation District (Texas) and cooperating irrigation farmers.

The ongoing research (1984-1985) of W-163 participants is listed by states as follows. The majority of research was being performed in California, Colorado, Texas, Utah, and Washington.

Arizona. USDA ARS Water Conservation Lab in Phoenix (John Replogle and Bert Clemmens) and The University of Arizona in Tucson (Del Fangmeier)

currently are not active in surge irrigation research. Some field recirculating infiltration tests were performed, and an interest exists in developing automated siphon tubes. The University of Arizona made available a 300-ft precision border for possible use by other W-163 members. A hydrodynamic model for border irrigation was developed by Theodore Strelkoff under the auspices of ARS in Arizona. This model is currently being used at The University of Texas at Austin.

California. The University of California at Davis (Wes Wallendar) is actively researching the effect of spatial variability in furrow irrigated field and application of the zero inertia model to surge flow irrigation.

Colorado. Colorado State University (Terrance Podmore) has been very active investigating the effect of surge flow on infiltration and advance. A kinematic wave model has been adapted to surge flow, and a step function surge flow infiltration model was developed.

Idaho. USDA ARS lab at Kimberly (Allan Humphreys and Tom Trout) is active in work with Utah and Colorado dealing with the hardware (valves and controllers) associated with surge flow irrigation, and in using laboratory and field test to study the effect of surge flow on infiltration.

Montana. Montana State University (Gerald Weston) developed a passive automatic culvert gate for surging water from a small reservoir into borders, and advance rates for surge flow in borders is being investigated.

New Mexico. New Mexico State University (Robert Hulsman) studied surge flow advance rates in borders.

Oklahoma. Oklahoma State University (James Garton) developed an automated ditch check surge system utilizing hooded ports installed in a trapezoidal concrete ditch. Infiltration and advance data were collected for one field site.

Oregon. Oregon State University (Marshall English) was proposing to investigate optimization methods for surge irrigation system design. However the current status of this effort was not reported at the last W-163 meeting in January of 1985. A limited number of field advance rate test were performed for cycle ratios of 1/3 and 2/3.

Texas. The SCS at Temple (Gene Lindeman) will be conducting field trials to compare surge irrigation using a constant versus variable cycle time. The Texas Agricultural Extension Service at Fort Stockton (Joe Hennegler) plans to undertake a water use efficiency field study of surge versus conventional furrow irrigation. Texas A&M University at College Station (Don Reddell) is currently developing a microcomputer controlled surge furrow irrigation system which senses the advance rate and transmits this information to the computer. The software uses a volume balance model presented by Reddell (1981).

Utah. Utah State University (Wynn Walker and Glenn Stringham) is active in developing an infiltration and hydrodynamic model of surge flow irrigation, and hardware systems for surge flow. Several of the

hydrodynamic models are being evaluated or used by the majority of W-163 participants, including Texas.

Washington. Washington State University (Day Bassett and Robert Evans) is investigating surge flow system hardware and the effect of surge flow on soil erosion.

D.3 Publications as a Result of This Research.

Only a small number of the previous national and international research publications concerning surface irrigation hydraulics have dealt with surge flow. Most of these reported observations from field tests. None of the studies have presented conclusive quantitative evidence explaining the reasons for the observed improvement in irrigation distribution efficiency with surge flow. Since the initiation of this research project in July, 1983, the following four articles have been written as a direct result of USGS funding. The published articles are:

1. "An Infiltration Model for Surge Flow," Proceedings of 1984 ASCE Irrigation and Drainage Division Specialty Conference, Flagstaff, Arizona, July 1984. pp. 691-700.

2. "Effect of Wetted Perimeter on Infiltration in Furrows," Proceedings of the 1985 ASCE Irrigation and Drainage Specialty Conference, San Antonio, Texas, July 1985, pp. 162-169.

3. "Effect of Surge Cycle Ratio and Cycle Time on Infiltration," Proceedings of the 1985 ASCE Irrigation and Drainage Specialty Conference, San Antonio, Texas, July 1985, pp. 154-161.

4. "Design and Calibration of a 200-ft Model Irrigation Border with a Computer Controlled Infiltrating Bed," Proceedings of the 1985 ASCE Hydraulics Division Specialty Conference, Orlando, Florida, August 1985, pp. 1310-1315.

E. METHODOLOGY

The effects of infiltration on surge flow furrow irrigation were investigated considering the hydrodynamics of free surface and porous media flow. There are four concerns: **a)** description of the physical system and flow process; b) mathematical and numerical modeling of hydrodynamics and infiltration; **c)** procedures of the design method; and **d)** design and calibration of a physical hydraulic model of an irrigation border/furrow.

E.1 Physical System and Flow Process

The physical system necessary to investigate the hydrodynamics of surge flow furrow irrigation must provide for control and/or measurement of ten functions:

1) Profiles of the advancing wetting front in the furrow

2) Recession of ponded water after the irrigation
3) Infiltration of water into the soil surface
4) Storage of water above the soil surface
5) Runoff or ponding of water at the end of the furrow
6) Furrow slope
7) Furrow surface roughness
8) Furrow cross-sectional geometry
9) Wetted cross-sectional perimeter
10) Inflow hydrograph

Figure 1 shows the surface and infiltration profiles in a furrow. The surface profile advances towards the end of the furrow, and the infiltration profile advances downward and toward the end of the furrow. The exact shapes of the profiles are predicted from hydrodynamic mathematical models and verified with experimentally determined data. Irrigation efficiencies relate to the shape and magnitude of the infiltration profile.

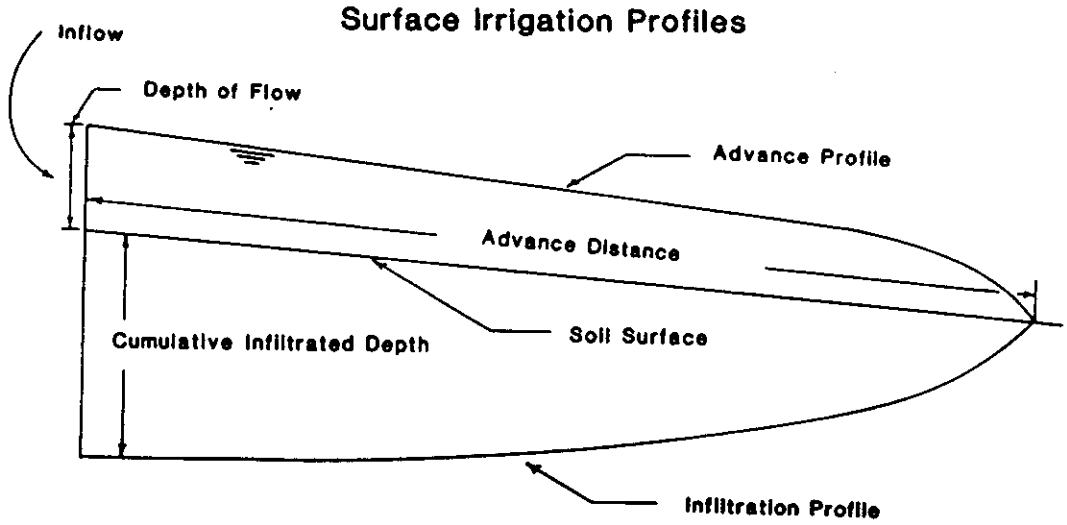

Figure 1 Surface and Infiltration Profiles

Advance and Recession Profiles. When water is applied to the furrow, part of the inflow infiltrates and the rest remains as surface storage and advances down the furrow. The advance is affected by many physical processes including furrow slope and roughness. However, the inflow rate and the infiltration characteristics of the soil primarily determine the surface storage and the rate of advance.

Ideally, the water should advance rapidly so that the outlet of the furrow may start receiving water quickly and well before over-irrigation occurs at the inlet. Moreover, it would be ideal if the advance rate paralleled the recession rate after the inflow is stopped. Therefore, any method of effectively quickening the wetting front advance by changing the hydrodynamics of the overland flow (through surge flow) or favorably altering infiltration characteristics will improve surface irrigation distribution efficiency.

Recession and advance can be occurring simultaneously at several longitudinal locations in the furrow or border during surge flow irrigation. A useful analogy for surge flow is to consider the surges as a pulse train were the amplitude is a hydraulic variable (flow rate, depth, flow area, mean velocity) and the pulse length is the advance distance for each unique surge. The amplitude of the surge is attenuated as it advances and the pulse length modulated with time and distance. Furthermore, one surge may overtake a previous surge and the surface flows coalesce. All of these physical possibilities must be accounted for in the mathematical model of surge flow.

Infiltration. Infiltration chacteristics in a heterogeneous soil vary with space and time. Factors of importance to infiltration are the soil texture, structure, type of clay, and cations associated with the clay. Some factors are relatively static while others change. Soil changes cause seasonal variations in the infiltration characteristics. Reasons for these changes include cultural practices and the related soil compaction, growth or deposition of vegetation, and biological or microbial effects.

Overall, infiltration characteristics are somewhat transient. Many are not controllable and are beyond the scope of this research. However, as suggested earlier, some change in infiltration may result from surge flow, and this was carefully analyzed in this research. Explanations for observed results in the field are provided and verified using controlled experiments.

Two significant results were the development of a surge infiltration model and an empirical equation which describes the effect of wetted perimeter on infiltration in furrows. These results are of critical importance to the surge flow design methods and the surge flow computer model developed under this project.

Surface Storage and Runoff. Surface storage is determined by using mathematical relationships based on the water surface profile and the cross-sectional shape of the model furrow. Surface storage and the recession of water after the inflow is stopped are important to irrigation efficiency. The runoff (or tail-water) is lost unless a return flow system is installed. Furrows may be blocked at the end to pond water, but in many cases much of this water will ultimately be lost to percolation below the root zone. Surge flow irrigation systems may have the potential for controlling this runoff loss by varying the surge cycle time and ratio.

Slope and Roughness. Small changes in magnitude of a uniform furrow longitudinal slope does not appreciably affect advance and infiltration characteristics. However, nonuniform slopes can greatly affect advance and, therefore, irrigation efficiency.

Furrow roughness will affect the advance profile; however, the effects have not been studied in detail. The furrow roughness changes significantly between the first and second irrigation after cultivation. However, numerical simulation of furrow irrigation has shown the effects of roughness to be minor except when excessive vegetation or debris is in the furrow channel, or roughness has a significant effect on flow depth which influences wetted perimeter and thus infiltration.

Wetted Perimeter and Furrow Shape. Infiltration into furrows has been shown to be a function of infiltration opportunity time and wetted perimeter of the furrow cross section by Samani (1984), Fangmeier and Ramsey (1978), Stelkoff and Souza (1985), and Blair and Smerdon (1985a). During the advance phase of furrow irrigation the wetted perimeter at a given longitudinal location rapidly increases with time and then slightly decreases after a static period (Strelkoff and Souza 1985). The slight decrease may be due to a reduction in furrow roughness with an increased conveyance capacity permitting a reduced flow depth. Because wetted perimeter is not static during an irrigation, the infiltration opportunity time changes not only with distance down the furrow, but also in relation to the transverse position within the furrow. Capillary effects induce a wetted fringe above the water surface. This portion of the cross section is not submerged, but the soil moisture content is increasing, thus affecting infiltration at a later time should this fringe become submerged. Also, anisotropy in soil may exist in relation to the furrow cross section. Thus, the infiltration rate may increase as a nonlinear or step function of wetted perimeter. In addition to the spatial variability of soil properties, infiltration in furrows can be influenced by infiltration in adjacent furrows. At a sufficiently long infiltration opportunity time, the horizontal wetting front from adjacent furrows will meet. Thus the combined effect of wetted perimeter and furrow geometry may vary with furrow spacing and infiltration opportunity time.

Surge flow irrigation further complicates the effect of wetted perimeter on infiltration by producing a discontinuous decrease in infiltration rate and thus a potential increase in wetted perimeter for surges subsequent to the first surge. During an actual surge irrigation, there exists a portion of the furrow wetted by advancing water during the off time. This section of the furrow has a much smaller wetted perimeter than the rest of the upsteam furrow, and this must be accounted for when calculating infiltration for the next cycle period. The dynamic nature of the wetted perimeter and the anisotropies present in the furrow cross section suggest that cumulative infiltration can be expressed by integrating an infiltration function over the wetted cross-sectional surface of the furrow. This can be expressed as

$$Z = \int_{-\frac{1}{2}P}^{+\frac{1}{2}P} f(\tau)\, ds \qquad (1)$$

where τ is infiltration opportunity time for a specific position s along the transverse of the furrow, P is the wetted perimeter of the furrow, and Z is the cumulative infiltration per unit length of the furrow. The function $f(\tau)$ is not easily formulated and must account for the dynamic effects of wetted perimeter. Several empirical equations were evaluated as alternatives to formulating $f(\tau)$. These equations and detailed results are provide by Blair and Smerdon (1985a). Overall, the results indicated that the Kostiakov cumulative infiltration equation, $Z = k\tau^a$, modified to include wetted perimeter raised to a power, appeared to satisfactorily represent the effect

of wetted perimeter on infiltration. The equation suggested is

$$Z = k\,\tau^{a}\,P^{b} \qquad (2)$$

where P is wetted perimeter, and k, a, and b are empirical coefficients.

As mentioned earlier, the effect of wetted perimeter on infiltration is a function of infiltration opportunity time. Thus equation (2) is most accurate during the intial infiltration period and its accuracy is likely to decrease with increasing infiltration opportunity time as other factors increasingly enter the picture. An alternative method would be to use a branch function similar the method suggested by Clemmens (1983). The difficulty in using a branch function is in defining the infiltration opportunity times at which the branch function changes. This difficulty is compounded by the fact that if the effect of wetted perimeter on infiltration is a function of both τ and P, and if equation (2) is used to describe this effect, then statistically determining the time at which P has little effect on Z requires a minimum of three infiltration tests at different wetted perimeters and a more sophisticated analysis method than ordinary multivariate least squares. Also, because the wetted perimeter is held constant during the infiltration test, and in reality wetted perimeter is a function of time during an actual irrigation, a bias may be introduced.

Furrow shape, in itself, may not significantly influence advance or infiltration characteristics, although the wetted perimeter (which is a function of flow depth and furrow shape) is recognized as being very important. Furrows are usually parabolic in cross-sectional shape and can be described using a power relationship function. The furrow shape will usually change during the first irrigation after cultivation. This change is related to erosion and sediment transport in the furrow. Assuming the furrow cross section is symmetric, then the furrow shape (Figure 2) can be represented by

$$y = \mu_1 x^{\mu_2} \qquad (3)$$

where x is the transverse (horizontal) distance from the center line of the furrow, y (positive upward) is the vertical height of the soil surface above the furrow bottom, and μ_1 and μ_2 are empirical coefficients. Wetted perimeter is equal to twice the arc length of equation (3), as given by

$$P = 2\int_0^{\frac{1}{2}B} \left[1+\left[\frac{d(\mu_1 x^{\mu_2})}{dx}\right]^2\right]^{\frac{1}{2}} dx = 2\int_0^{\frac{1}{2}B} \left[1+(\mu_1\mu_2)^2 x^{2(\mu_2-1)}\right]^{\frac{1}{2}} dx \qquad (4)$$

where P is the wetted perimeter, μ_1 and μ_2 are coefficients, and B is the water surface width (top width). Equation (4) is difficult to analytically integrate for noninteger values of μ_2; however it can be easily solved numerically.

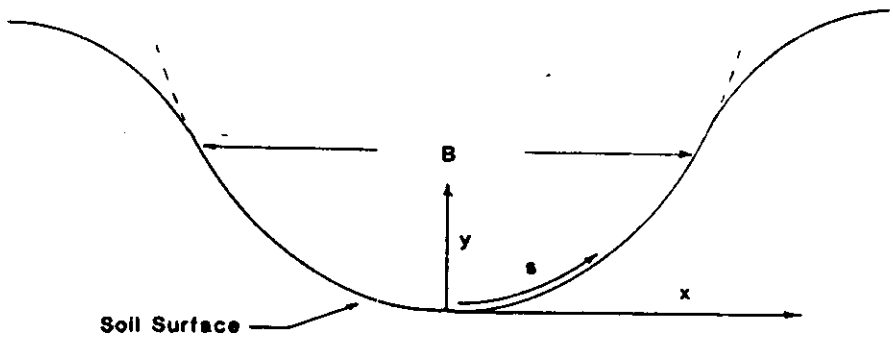

Figure 2 Power Function Shaped Furrow Cross Section

Surge Inflow Hydrograph. The subsection, **Definition of Surge Flow,** in section B of this report defines the inflow hydrograph as a function of surge cycle ratio, cycle time, and valve sequencing pattern (VSP). Currently the functional form of the optimal VSP is not known. As previously stated, most commercial surge flow systems use a constant cycle ratio, r, and cycle time, t_c. Thus, the VSP is constant. However, limited field data and computer simulations indicate that the VSP is a nonlinear, unimodal function. In achieving an optimal design the VSP function will have to be related to the cycle ratio and cycle time.

In addition to the continuous functions for t_c and r, it is likely that a step function is appropriate to account for the transition between the advance phase and the continuation (cut back) phase of irrigation. The continuation phase begins when runoff first occurs.

E.2 Mathematical Modeling

The mathematical modeling concerns two distinct areas of research. First, the modeling of the hydrodynamics of surge and continuous furrow irrigation; second the modeling of infiltration or porous media flow. Both a hydrodynamic model and an infiltration model are required to model surge or continuous irrigation; however, several types and combinations of models are possible. The following sections explain the various models.

Hydrodynamic Models. The three hydrodynamic models which were evaluated are: a) kinematic wave; b) zero inertia; and c) full dynamic wave. Because of its applicability to surge flow, the kinematic wave model was selected for use preliminary design of surge irrigation system, and is the only model which is discussed and derived in this report. Results from the kinematic wave model are presented in the **Principle Findings** section of this report.

Kinematic Wave Model. The kinematic wave or normal depth model (Walker and Humphreys, 1983) solves the continuity equation (5) and assumes a normal depth momentum equation (6). These are

$$\frac{\partial Q}{\partial x} + \frac{\partial A}{\partial t} + \frac{\partial Z}{\partial t} = 0 \qquad (5)$$

$$S_b = S_f \qquad (6)$$

where, **A** = cross-sectional area, **Q** = inflow rate, **Z** = infiltrated volume per unit furrow length, **x** = distance from inlet of furrow, **t** = time, S_b = bed slope, and S_f = the slope of the hydraulic grade line.

The major assumption made in solving equation (6) is that inflow rate and flow area in the furrow are uniquely related by Manning's uniform flow equation (7). Therefore, if equation (5) and (6) are solved using a finite difference method, the flow is assumed to be at normal depth in a piece-wise discrete manner. Manning's equation is assumed to fit a form of a power equation (9). Manning's equation requires that the furrow have a slope greater than zero and neglects any backwater effects. The coefficients for Manning's equation are determined by the furrow shape and roughness. Manning's equation is:

$$Q = \frac{1}{\eta} \frac{A^{5/3}}{P^{2/3}} S_b^{1/2} \qquad (7)$$

where η is Manning's roughness coefficient. Assuming that wetted perimeter and flow area are related by

$$P = \omega_1 A^{\omega_2} \qquad (8)$$

then equation (7) can be written as

$$Q = \alpha_1 A^{\alpha_2} \qquad (9)$$

$$\text{with} \quad \alpha_1 = \frac{S_b^{\frac{1}{2}}}{\eta\, \omega_1^{2/3}} \qquad (10)$$

$$\text{and} \quad \alpha_2 = 5/3 - 2/3\omega_2 \qquad (11)$$

where ω_1 and ω_2 are empirical coefficients. Determination of ω_1 and ω_2 can be made by using equations (3) and (4). The procedure requires numerical solution of equation (4) and least squares fitting of equation (3). The coefficients μ_1 and μ_2 in equation (3) are determined from field measurement of the furrow shape. Analytical solutions exist for the case when μ_2 is an integer equal to 1 or 2; however, these solutions are lengthy and require more effort to program into a computer than the numerical solutions.

The continuity equation and Manning's equation can be solved using the method of characteristics or numerical integration. The integration method is easier to adapt to surge flow. A deformable body of water with a moving reference coordinate system is used to describe the surface flow (Walker and Humphrey 1983).

The partial differential continuity equation (5) can be solved in an integral form which is

$$\iint \frac{\partial Q}{\partial x}\, dx\, dt + \iint \frac{\partial A}{\partial t}\, dt\, dx + \iint \frac{\partial Z}{\partial t}\, dt\, dx = 0 \qquad (12)$$

with limits of integration of x, $x+\Delta x$ and t, $t+\Delta t$. The first order approximation to the solution of equation (12) is

$$[\hat{Q}(x+\Delta x,t)-\hat{Q}(x,t)]\Delta t + [\overline{A}(x,t+\Delta t)-\overline{A}(x,t)]\Delta x + [\overline{Z}(x,t+\Delta t)-\overline{Z}(x,t)]\Delta x = 0 \qquad (13)$$

where overbar symbol $\hat{}$ denotes a temporally averaged variable over the interval Δt, and the overbar symbol $\bar{}$ denotes a spatially averaged variable over the interval Δx. A first order numercal integration (finite difference) method can be used to solve equation (13). The method proposed assumes that the averaged variables, Q, $\overline{A}$, and Z, can be replaced with the product of a nonaveraged variable and a weighting function which results in

$$\left[[(1-\theta)Q_i + \theta Q_j] - [(1-\theta)Q_{i-1} + \theta Q_{j-1}]\right]\Delta t + \left[[(1-\psi)A_{j-1} + \psi A_j] - [(1-\psi)A_{i-1} + \psi A_i]\right]\Delta x + \left[[(1-\varepsilon)Z_{j-1} + \varepsilon Z_j] - [(1-\varepsilon)Z_{i-1} + \varepsilon Z_i]\right]\Delta x = 0 \qquad (14)$$

where the spatial weighting functions are ε and ψ, and the temporal weighting function is θ ($0 \le \varepsilon \le 1$, $0 \le \psi \le 1$, $0 \le \theta \le 1$). Discussion of these weighting fuctions is provided by Cunge, Holley and Verwey (1980).

If the process defined by equation (12) is linear with respect to time and distance, then using $\varepsilon = \frac{1}{2}$, $\psi = \frac{1}{2}$ and $\theta = \frac{1}{2}$, results in equation (14) being an exact solution to equation (12). For $\varepsilon = \frac{1}{2}$, $\psi = \frac{1}{2}$ and $\theta = \frac{1}{2}$, equation (14) is defined as a trapezoidal rule method, however the most appropriate values of ε, ψ and θ are functions of i, j subsripts and the magnitudes of Δx and Δt in equation (14). The subscripts i, j, $i-1$, and $j-1$ are defined on finite difference grid illustrated in Figure 3.

For any nonlinear process if the selected values of Δt and and Δx are small enough, then using $\varepsilon = \frac{1}{2}$, $\psi = \frac{1}{2}$ and $\theta = \frac{1}{2}$ is appropriate. Strelkoff (1983) suggests that if the "discharge in the interior of the stream is sufficiently gradual and close to linear that the trapezodal rule" method can be applied; however, "near the boundaries of the surface stream ... variables can change rapidly and curvilinearly." The primary boundaries of concern are at the tip of the advancing stream, at the tail of the recesession stream, and at the interception of flow profiles (such as occurs when water ponds behind a blocked furrow). Strelkoff further suggests empirical functions based on the length of the cell (Δx) for ψ; and based on the exponent a in the Kostiakov cumulative infiltration equation for ε.

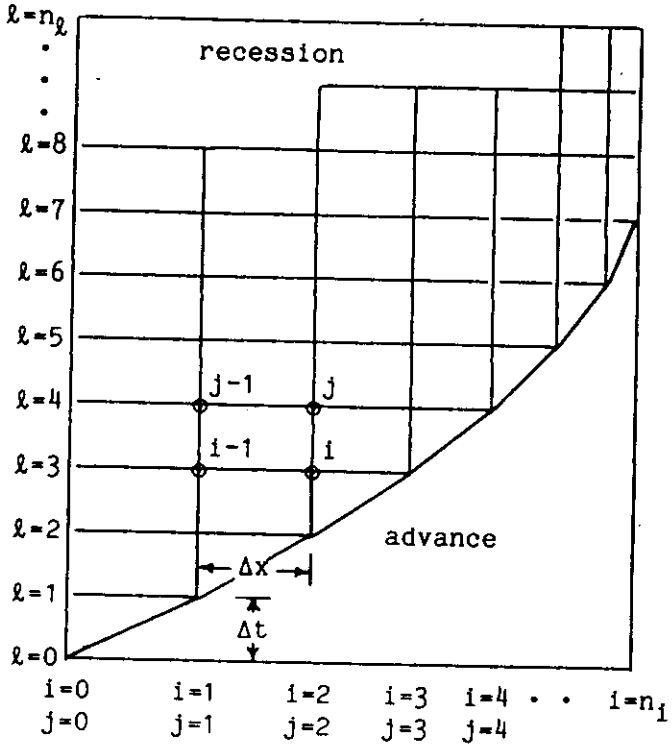

Figure 3 Finite Difference Grid

Solving equation (14) in terms of of the unknown variables A_j, Q_j, and Z_j results in

$$\theta Q_j \Delta t + \psi A_j \Delta x + \varepsilon Z_j \Delta x$$

$$+ \left[(1-\theta)Q_i - [(1-\theta)Q_{i-1} + \theta Q_{j-1}]\right]\Delta t$$

$$+ \left[(1-\psi)A_{j-1} - [(1-\psi)A_{i-1} + \psi A_i]\right]\Delta x$$

$$+ \left[(1-\varepsilon)Z_{j-1} - [(1-\varepsilon)Z_{i-1} + \varepsilon Z_i]\right]\Delta x = 0 \qquad (15)$$

Incorporation of equation (6) into the soultion of equation (5) is done by substituting $Q = \alpha_1 A^{\alpha_2}$ into equation (15) and simplifing in terms of the dependent variables, Q_j, A_j, and Z_j. This results in

$$\theta\alpha_1 A_j^{\alpha_2}\Delta t + \psi A_j \Delta x + \varepsilon Z j \Delta x$$

$$+ \left[(1-\theta)A_i^{\alpha_2} - [(1-\theta)A_{i-1}^{\alpha_2} + \theta A_{j-1}^{\alpha_2}]\right]\alpha_1\Delta t$$

$$+ \left[(1-\psi)A_{j-1} - [(1-\psi)A_{i-1} + \psi A_i]\right]\Delta x$$

$$+ \left[(1-\varepsilon)Z_{j-1} - [(1-\varepsilon)Z_{i-1} + \varepsilon Z_i]\right]\Delta x = 0 \qquad (16)$$

The cumulative infiltration variable Z_j is a function of both infiltration opportunity time τ and wetted perimeter **P**. The method used to calculate Z_j is based on the trapezoidal method of numerical integration of infiltration rate, $dZ/d\tau$, over the finite difference interval Δt. The equations describing this are

$$Z_j = Z_i + \left[\frac{dZ}{d\tau}\right] \Delta t \tag{17}$$

$$\left[\frac{dZ}{d\tau}\right] = \tfrac{1}{2}\left[k\, a\, (\tau-\Delta\tau)^{a-1}\, \omega_1^{b}\, A_i^{\omega_2 b} + k\, a\, \tau^{a-1}\, \omega_1^{b}\, A_j^{\omega_2 b}\right] \tag{18}$$

During continuous flow irrigation, the infiltration opportunity time, τ and $\Delta\tau$, are equal to

$$\tau = (\ell-j)\, \Delta t \tag{19}$$

$$\Delta\tau = \Delta t \tag{20}$$

where ℓ is defined by Figure 3. During surge flow irrigation, τ and $\Delta\tau$, must be calculated as the total time since water first ponds (i.e $A_{j-1} > 0$ or $A_j > 0$) at the $(j-1)^{th}$ and j^{th} finite difference nodes. Also, there exists a longitudinal section of the furrow which is wetted during the off period. This section of the furrow has a much smaller wetted perimeter than the rest of the upstream furrow. Walker and Humphrey (1983) used an power transition function to model this effect, and Izuno and Podmore (1984) used a branch transition function. The method proposed in this report consist of treating infiltration, Z_j, as a function of A_j, **r**, t_c, and τ. Modeling the transition is implicitly contained within solution of equation (16) if τ is both a function of the longitudinal and transverse location within the furrow. Walker and Humprey (1983) reported that this transition is of consequence only in the section of furrow effected by the subsequent surge. And if the increase in wetted perimeter is rapid with the onset of the next surge, then only two values of τ for each longitudinal location are necessary.

Numerical solution of equation (16) using a Newton-Raphson method requires the first derivative with respect to A_j which is

$$\theta\, \alpha_1\, \alpha_2\, \Delta t\, A_j^{\alpha_2-1} + \psi\, \Delta x + \tfrac{1}{2}\, \epsilon\, \Delta x\, \Delta t\, k\, a\, \tau^{a-1}\, w_1^{b}\, w_2\, b\, A_j^{w_2 b-1} = 0 \tag{21}$$

Equation (16) is the solution for an interior rectangular cell in the finite difference grid. During the initial advance of water over a dry soil, the finite difference cell which denotes the advancing tip of the water stream is triangular in shape. The variables A_{i-1}, A_i, A_j, Z_{i-1}, Z_i, and Z_j are all zero and equation (16) can be simplified to

$$-\theta Q_{j-1}\Delta t + \psi A_{j-1}\Delta x + \epsilon Z_{j-1}\Delta x = 0 \tag{22}$$

From equation (22), Δx can be solved directly as

$$\Delta x = \frac{\theta\alpha_1 A_{j-1}^{\alpha_2}\Delta t}{(\psi A_{j-1} + \epsilon Z_{j-1})} \tag{23}$$

In surges subsequent to the initial surge the soil may not be dry and coalescence of the current advancing surge with the previous receding surge may occur. For these situations the variables A_{i-1}, A_i, A_j, Z_{i-1}, Z_i, and Z_j may not be zero. Thus equation (23) may be invalid for surges which occur after the initial surge, and equation (16) should be used instead.

Initial and Boundary Conditions. The finite difference solution of equation (16) requires that the initial flow are A_i for $\ell=0$ be known. If the solution is for an initially dry furrow, then $A_i = 0$ for $i=1,n_i$ and for $i=0$

$$A_0 = \left[\frac{Q_{in_1}}{\alpha_1}\right]^{(1/\alpha_2)} \qquad (24)$$

where Q_{in} is the initial infow rate. The upstream boundary condition must be known and for surge flow irrigation it is defined by a function of cycle ratio and cycle time.

The kinematic wave model assumes a unique relationship between flow rate, flow area, and energy loss; thus any downstream boundary conditions are ignored. Also, since this unique relationship is assumed defined by Manning's equation, the accuracy of the results from the model are dependent on the value of S_b. The downstream boundary conditions can be modeled in two ways: as an unrestricted flow; and as a stagnet pond which has no effect on the stream of water entering the pond. The first condition is assumed during the advance phase of irrigation and if the water is allowed to runoff the field. The second condition is used if the end of the furrow is blocked, and the location of the interception of the water stream and the of the ponded water is calculated from furrow geometry and conservation of volume equations.

Infiltration Models. Izuno, Podmore, and Duke (1985), Blair, Smerdon, and Rutledge (1984) and Samani (1983) have developed infiltration models for surge flow. Samani's work pertained to the numerical solution of Richard's Equations for one and two dimensional porous media flow, and is overly complex for direct application to design procedures; hence this model is not discussed in this report.

Four reasons are proposed for the reduction in infiltration which occurs in surge irrigation: sealing due to expansion of the clay fraction in the soil as it hydrates, reduction in the hydraulic gradient as soil wetting proceeds, consolidation of the surface soil due to drying during the off-period, and sealing by clogging from sediment particles.

Cycle Ratio-Time Model. The model proposed by Blair, Smerdon, and Rutledge (1984) is based on the assumption that clay hydration and the reduction in hydraulic gradient accounts for the largest portion of the observed difference between continuous and surge flow infiltration. This model requires that the **k**, **a**, and **b** coefficients in equation (2) be obtained from field data.

This model is based on the assumption that the factors which reduce infiltration, as time progresses after initial wetting, continue to operate unabated during the off-period. The same reduction occurs during continuous irrigation, but at a different infiltration opportunity time than for surge irrigation. The difference in opportunity times is assumed proportional to the cycle ratio. The model implies that surge flow requires

less water than continuous flow to produce an equivalent reduction in infiltration, a reasonable expectation if the infiltration rate decreases as a function of time after the soil is initially wetted.

The variables in the model are defined as:

Z = cumulative infiltration per unit length of furrow for continuous flow
Z' = cumulative infiltration per unit length of furrow for surge flow
t_c = surge flow cycle time
r = surge flow cycle ratio
n = n^{th} surge flow period, n=0 is the 1st surge, n = 1 is the 2nd, etc.
k = coefficient for continuous flow infiltration equation
a = exponent for continuous flow infiltration equation
b = exponent for continuous flow infiltration equation
k' = coefficient for surge flow infiltration equation
a' = exponent for surge flow infiltration equation
P = wetted perimeter
i = i^{th} surge period out of n periods

Figures 4 through 6 illustrate this simple mathematical model for surge flow irrigation using the Kostiakov equation. Figure 4 shows a cumulative infiltration curve with the surge ON/OFF periods superimposed. Figure 5 shows the discontinuous curve produced when the cumulative infiltration is removed during the OFF periods. Figure 6 shows the resulting cumulative infiltration during the surge ON times. The time axis in Figure 6 represents compressed time or cumulative ON time, not real time. Also note, the height of the surge flow curve in Figure 6 is less than height of the continuous flow curve. This means that for any given compressed time (time when water is turned on) during surge flow the cumulative infiltrated volume will be less than for an equivalent real time during continuous flow.

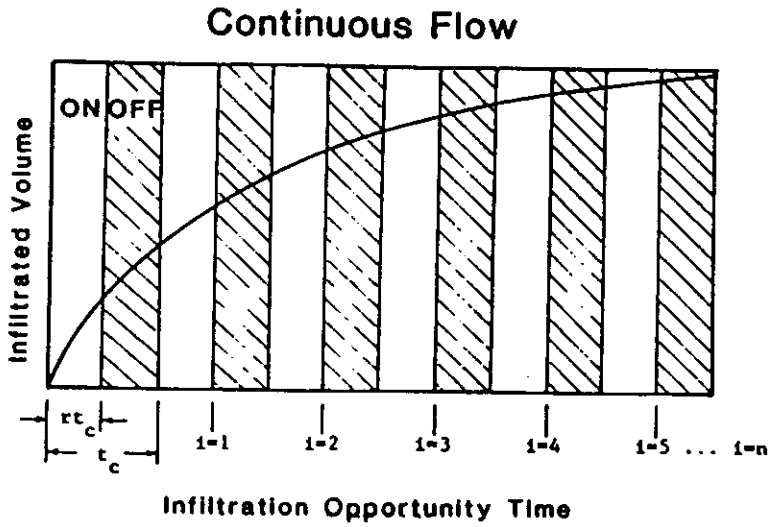

Figure 4 Continuous Flow Cumulative Infiltration Curve

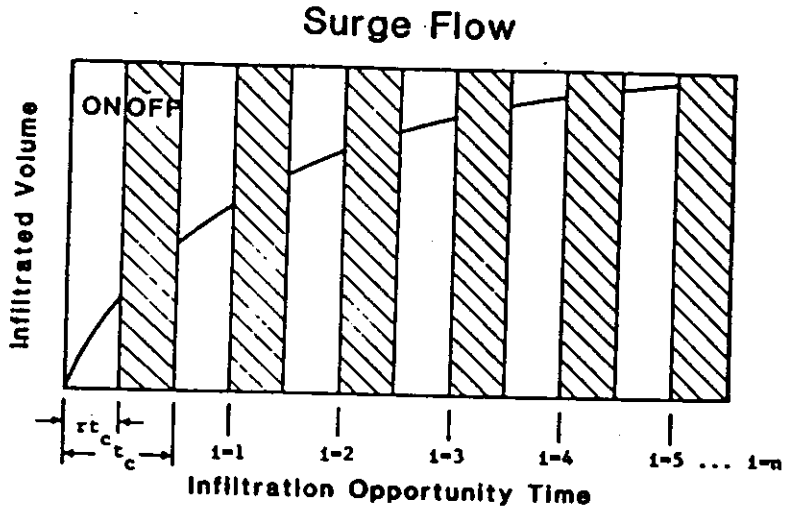

Figure 5 Continuous Flow Cumulative Infiltration Curve With Infiltration Which Occurs During Surge Off Periods Removed

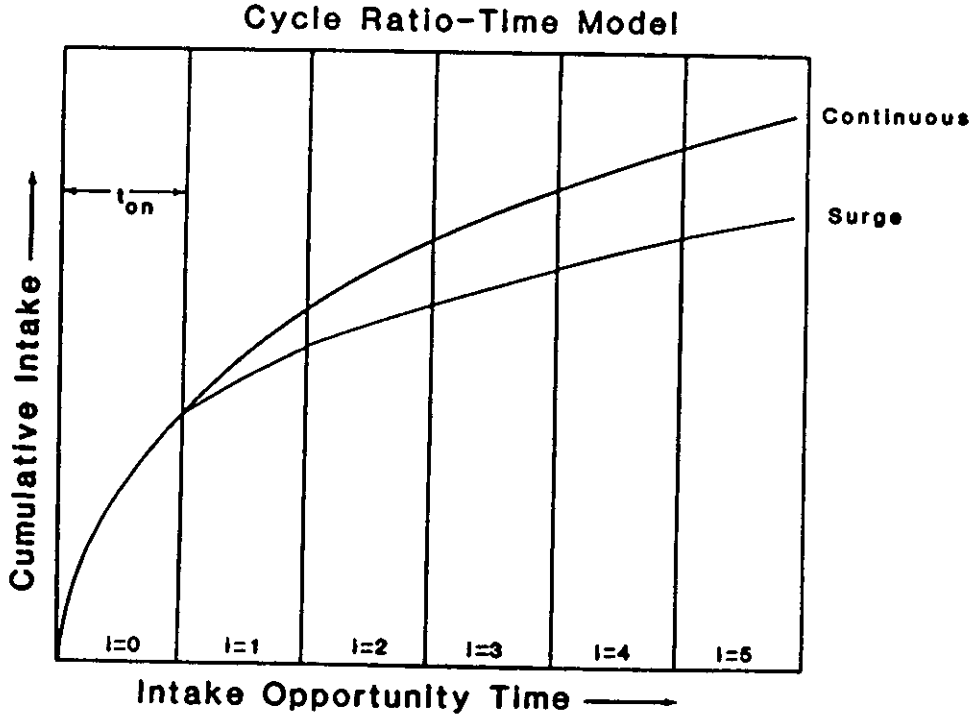

Figure 6 Continuous and Surge Cumulative Infiltration Curves

For any given k, a, r, and n there are n+1 values of k' and a' coefficients that can be derived. This results in a different k' and a' value for each previously wetted section of the furrow during the sequences of surges. Each section of the furrow has a k' and a' value related to the number of surges which has passed over that section. The continuous values, k and a, and the surge flow values, k' and a', are identical for the first surge where i = 0. The k' and a' values in the remaining surges, i = 1, 2, 3, ... n are derived assuming that the surge flow infiltration volume equals the equivalent continuous volume minus the volumes that would have infiltrated during the off periods. This leads to:

$$\frac{Z'_n}{p^b} = \frac{k}{p^b} \sum_{i=0}^{n} \left[(rt_c + it_c)^a - (it_c)^a\right] \qquad (25)$$

Rearranging Z'_n in terms of k'_n and a'_n and canceling p^b results in

$$k'_n \left[(n+1)(rt_c)\right]^{a'_n} = k \sum_{i=0}^{n} \left[(rt_c + it_c)^a - (it_c)^a\right] \qquad (26)$$

In Figure 6 the surge and continuous infiltration are identical up to a time of $t = rt_c$ which corresponds to $n = 0$. Therefore, k'_n for $n = 0$ can be written as

$$k'_0(rt_c)^{a'_0} = k(rt_c)^a \qquad (27)$$

This simplifies to $$\frac{k'_0}{k} = (rt_c)^{(a-a'_0)} \qquad (28)$$

Since both the surge and the continuous infiltration curves must pass through the point $Z = Z'$ at $t = t_c$, the surge infiltration equation should be forced through that point. This can be done by substituting equation (28) into equation (26) for $n = 0$. The result is

$$(n+1)^{a'_n}(rt_c)^a = \sum_{i=0}^{n} \left[(rt_c + it_c)^a - (it_c)^a\right] \qquad (29)$$

Cancelling t_c and rearranging results in

$$r^a (n+1)^{a'_n} = \sum_{i=0}^{n} \left[(r + i)^a - i^a\right] \qquad (30)$$

Taking the logarithms of equation (30) and rearranging results in

$$a'_n = \frac{\ln\left[\sum_{i=0}^{n} \left[(r + i)^a - i^a\right]\right] - \ln(r^a)}{\ln(n + 1)} \qquad (31)$$

The value of a'_n can be substituted into equation (28) to find the value of k'_n.

The surge flow coefficients **k'** and **a'** are dependent on the cycle ratio, **r**; the continuous flow coefficients, **a** and **k**; and the number of surge cycles, **n**. This has the effect of producing a different value for **k'** and **a'** for each surge cycle. The values in Table 1 illustrate the procedure and were determined from equations (25) and (31) using arbitraty values of p^b = **1, a = 0.6, k = 1.5, r = 0.5** and t_c = **30** minutes. The **k'** and **a'** values associated with the limit of equation (31) as $n \to \infty$ define a surge flow infiltration curve shown in Figure 6. The values of **k'** and **a'** for a large value of **n** are approximately equal to the values for the limit of equation (31).

Table 1 Surge Flow Coefficients k' and a'

n	a'	Δa'	k'	Δk'
0	0.600	---	1.50	---
1	0.503	---	1.949	---
2	0.508	0.005	1.926	0.023
3	0.511	0.003	1.909	0.017
4	0.514	0.003	1.900	0.009
5	0.516	0.002	1.884	0.006
10	0.523	0.001	1.847	0.007
100	0.546	0.00026	1.737	0.001
1000	0.561	0.000017	1.667	0.00008
10000	0.570	0.0000009	1.627	0.000004

Soils with Kostiakov infiltration equations which have small values of the exponent a in the Kostiakov equation are soils with highly nonlinear infiltration rates. These are soils in which the influence of clay expansion sealing and hydraulic gradient reduction would be expected to play the major role. Therefore, these are the soils in which we anticipate that the suggested model would account for the largest portion of the observed difference between continuous and surge flow infiltration. Although sufficient data are not available to verify such a conclusion, the data obtained so far leads us to believe that it may prove possible to improve the accuracy of the model by adjusting the model based on the value of the a exponent. However, such a modification must await more experimental data.

Step Function Model. Izuno, Podmore and Duke (1984) suggested a surge flow infiltration model based on a modified version of the Kositakov equation. This model is based on data collected from a silty clay loam field with **r** = 0.5 and t_c = 60 minutes. The model assumes that during the first cycle, infiltration rate is controlled by the nonlinear term, $\tilde{k}t^{\tilde{a}}$, and for all subsequent surges the infiltration is determined by the linear term, $\tilde{c}t$. The model assumes that a constant infiltration rate is achieved after one cycle period, as illustrated by Figure 7. In this model infiltration is not a function of cycle ratio, and is

$$Z = \tilde{k}\, t^{\tilde{a}} \qquad \text{for} \quad t \leq t_{on}, \text{ and} \tag{32}$$

$$Z = \tilde{k}\, t_{on}^{\tilde{a}} + \tilde{c}\,(t - t_{on}) \qquad \text{for} \quad t > t_{on} \tag{33}$$

where **t** is the cumulative infiltration opportunity time, Z is cumulative infiltration, and t_{on} is the duration of the first surge ON period.

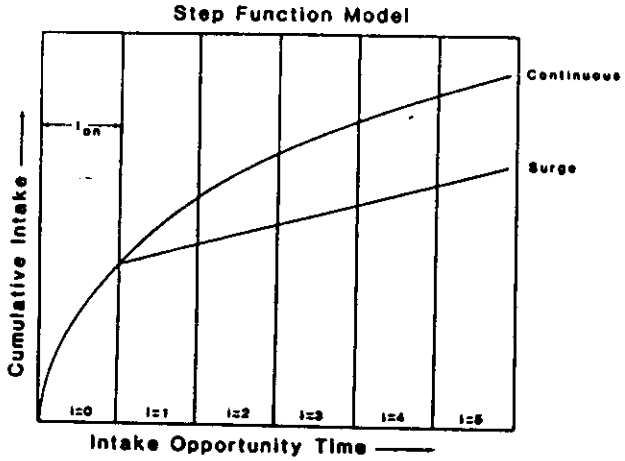

Figure 7 Step Function Surge Flow Infiltration Model

E.3 Design Methods.

Dimensionless respresentation of variables often used in irrigation design methods to reduce the number of design parameters and to present the results of the analysis in a form representative of a common base. Souza (1980) provides a detailed discussion of the dimensionless solution of the Saint Venant equations for continuous flow furrow irrigation. Souza's approach is very useful for the theoretical analysis of furrow irrigation performance. However, on-farm applications of dimensionless methods may be confusing to some potential users of the design method, and often the use of dimensions is preferred. The kinematic wave model outlined in this paper uses dimensioned variables, and was designed for use by extension engineers and engineers in practice.

The typical user of this model is intereseted in obtaining the cycle ratio, cycle time, number of surges, and inflow rate which produces an optimal efficiency for a specific irrigated field. The model requires a trial and error method for finding these optimal parameters. Currently, additional research is being performed to develop a computer model which automatically optimizes the solution.

The hydraulic variables required for the kinematic wave model are:

Q_{in} = flow rate at the inlet to the furrow
L = field length
S_b = longitudinal field bed slope (assumed uniform throughout field)
k,a,b = empirical infiltration coefficients
μ_1, μ_2 = empirical furrow shape coefficients
n = Manning's roughness coefficient
t_c = surge flow cycle time
r = surge flow cycle ratio
d = desired application depth of water at tail-end of furrow
t_i = maximum time of irrigation (cumulative time water is on)

Typical input to and output from the kinematic wave model, and the specifications for the hydraulic and numerical variables used in the model are listed in Appendix B, **Surge Flow Kinematic Wave Furrow Irrigation Model.**

E.4 Experimental Procedures.

The experiments where grouped into two categories: a) physical modeling experiments; and b) field infiltration tests.

Physical Modeling. A unique part of this research was the development of a large scale computer controlled model border/furrow and infiltration simulator. The model furrow infiltration simulator was built using a long tilting flume. This flume is 61 meters long by 0.76 meters wide by 0.61 meters deep. Figure 8 shows a photograph of the flume. The vertical boards shown in Figure 8 were used as wind breaks. The outdoor flume is located at the Center for Research in Water Resources, The University of Texas at Austin. Typical borders and furrows are 200 to 400 meters in length and ideally a flume of similar length should be used. However, the 61 meter physical model is of sufficient size to be considered a full scale model. The physical model was constructed because field irrigation experiments are often imprecise and labor intensive. Also, the model can precisely control and measure infiltration, roughness, slope, bed uniformity, channel geometry, and water surface profiles. The model is converted from a border to a furrow by placement of a furrow shaped urethene mold on top of the gravel bed.

The model border shown in Figure 8 and described herein was built using a gravel bed. The bed was partitioned below the surface into fifteen sections, each 4.06 meters long. Each section contains a buried inlet header connected to a computer controlled submersible pump, and an electronic water depth sensor. These partitioned sections were used to simulate infiltration. The bed slope was adjustable between 0.0 and 0.0032 m/m, the maximum inflow rate was 3.0 liters/second and the maximum simulated infiltration rate was 4.0 mm/minute. The bed material was graded gravel with an equivalent mean spherical diameter of 13.5 mm, and the average Mannings n was 0.019 measure when the slope of the flume was for 0.0032 m/m and a flow rate of 2.5 liters/second during a test with no infiltration.

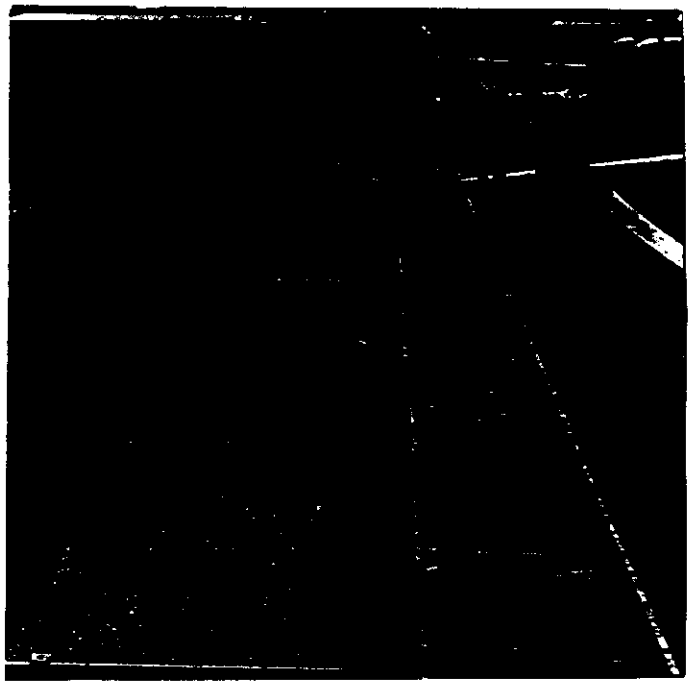

Figure 8 Model Border/Furrow

Instrumentation. The instrumentation of the model border consisted of two types: the hardware installed in the flume and the data acquisition and process control systems. The hardware in the flume consisted of the infiltration simulators outlined in Figure 9, the water depth sensor shown in Figure 10, and various flow rate measuring and control devices. Figure 11 shows the components which make up the data acquisition and process control system.

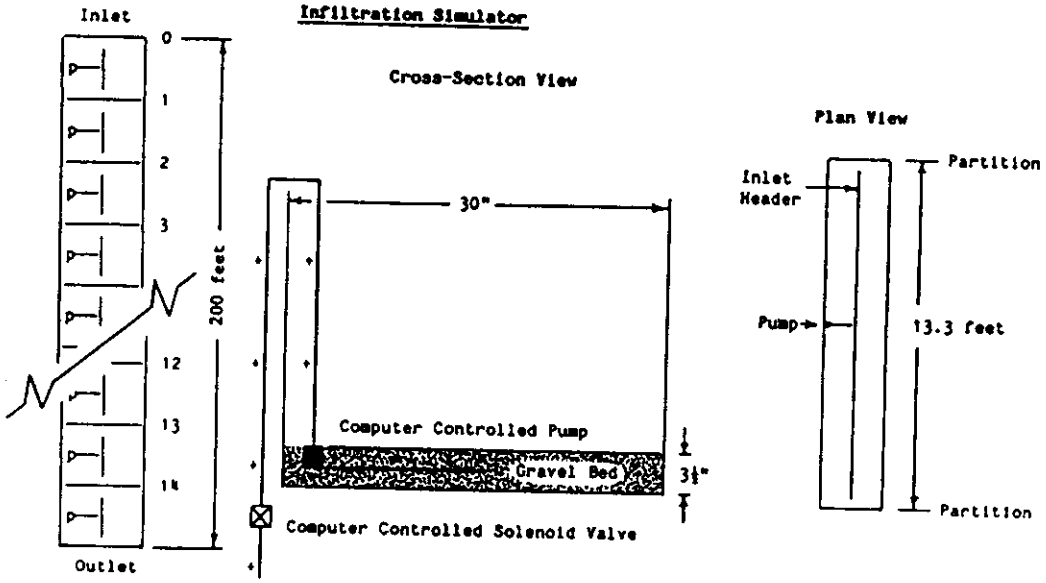

Figure 9 Infiltration Simulator

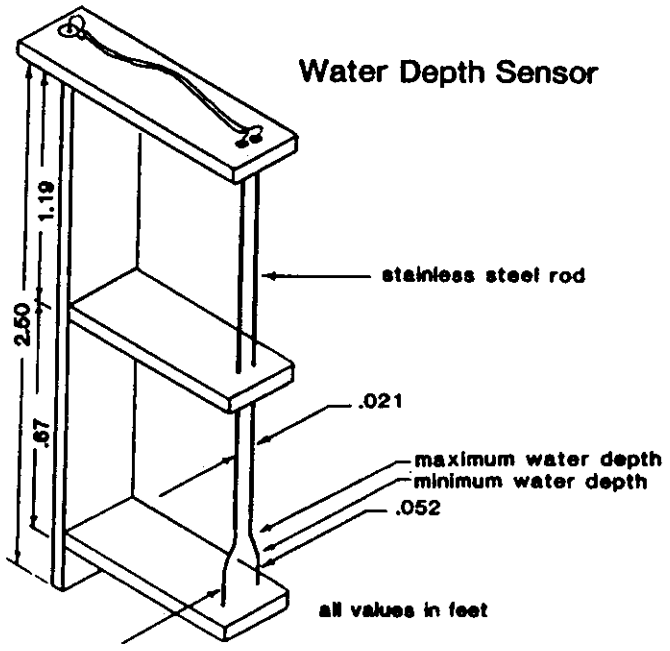

Figure 10 Water Depth Sensor

The data acquisition and process control system consisted of two microcomputer systems and several peripheral devices. A sine wave generator was used to excite the water depth sensors, and the potential drop was measured using a resistor bridge and a digital voltmeter. A multiplexor was used to scan the 15 sensors. The minimum scanning time was approximately 1 second per 15 sensor readings. However, it turned out that more accurate readings were obtained by increasing the integration time of the RMS convertor in the digital voltmeter to 1/6th second which produced a scan time of 4 seconds for 15 sensors. The data acquisition computer calculates the infiltration rate for each simulator based on depth measurements and relays the rate to the process control computer via a hardwire interrupt and an asynchronous serial interface.

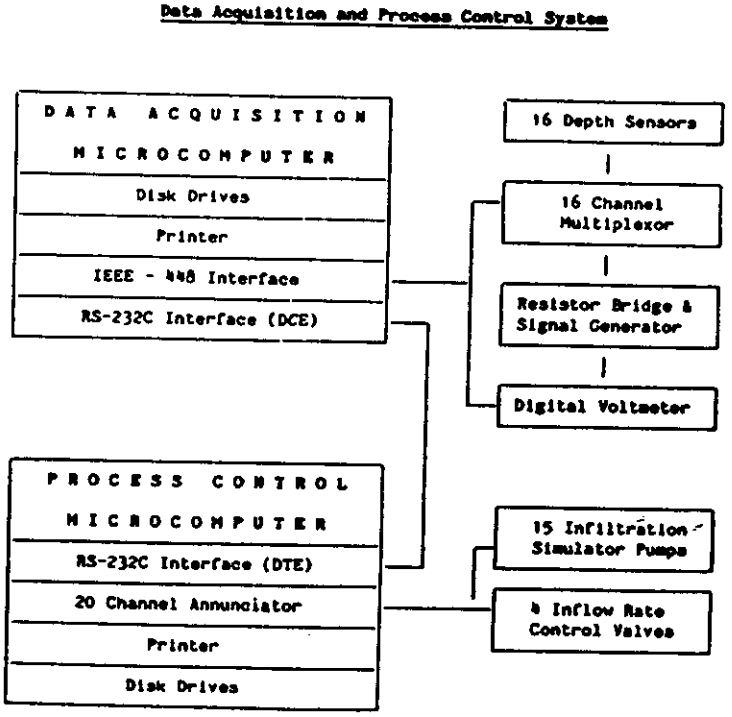

Figure 11 Data Acquisition and Process Control System

The water depth sensor was designed to be simple and produce a linear function of RMS voltage versus depth of flow. This function can be affected by: water conductivity, water temperature, the contact angle of the water on

the stainless steel rods, mineral deposits, and signal grounding. Because of these many factors each sensor is automatically calibrated prior to every experiment. The water depth sensor used was similar in design to those used by Wessels and Strelkoff (1968), except the distance between the pair of wires decreases as flow depth increases (as shown in Figure 10). This was done to make the response of the sensors more linear.

Simulated Infiltration. The process control computer simulates infiltration by rapid pulsing of submersible pumps buried in the gravel bed of the flume. The simulated infiltration rate is an empirical function of the cycle time and cycle ratio for the pump. Thus, simulated infiltration is both discrete in space (15 simulators) and in time (pulsing). Ideally, the simulated discrete infiltration would approach real continuous infiltration if the number of simulators was large and the on-time was small. Practical limitations in control, measurement, and cost required a maximum of 15 simulators, and a minimum on-time of 2 seconds. Infiltration during surge flow irrigation is modeled using the cycle ratio-time model developed in this report.

Simulated infiltration is also a function of the amount of time required to receive infiltration rates from the data acquisition computer and how often the data acquisition computer updates the rates. Ideally, the process control computer would receive the rates instantaneously and be updated continuously. Practicality required a 0.8 second receive time and 12 seconds between updates.

The infiltration simulation software was designed to minimize the difference between the continuous and discrete cumulative infiltration. Figure 12 shows the continuous infiltration rate superimposed over the associated discrete infiltration rate. The algorithm which simulates infiltration must consider both the discretization in time and location of the water depth sensors within the partitioned sections of the infiltration simulator.

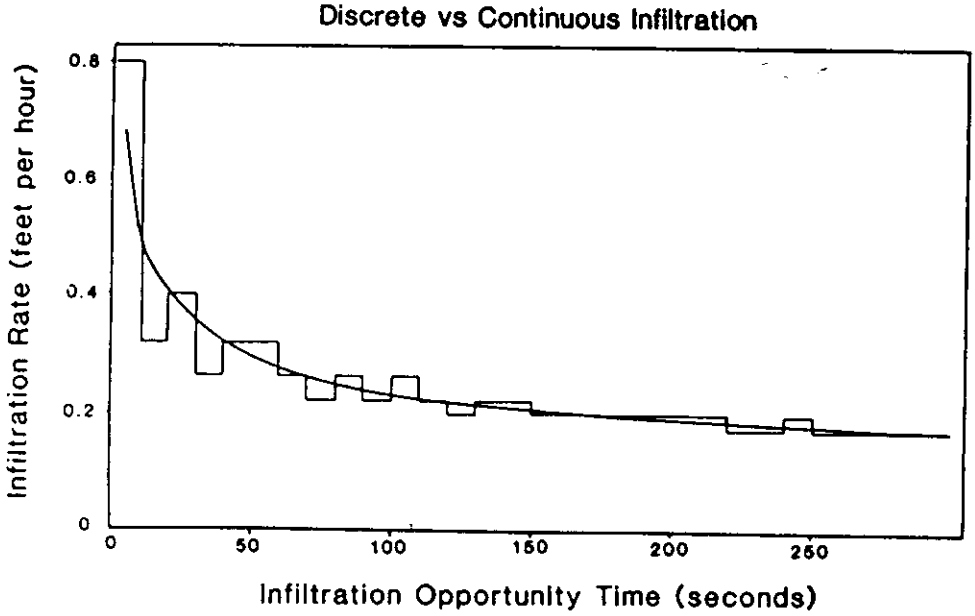

Figure 12 Discrete and Continuous Infiltration Rate

Calibration. The inflow control valves and the infiltration simulators were calibrated using volumetric and weighing methods. The gravel bed was made uniform by floating a horizontal board over the bed. The elevation of the board was controlled by using the top of the flume sidewall as a reference. The water depth sensors were calibrated using piezometers and steady flow conditions. The corresponding RMS voltage readings for the steady flow conditions were automatically measured prior to each experiment. During an experiment the actual depth of flow was determined by measuring the RMS voltage and interpolating between steady flow values. Slight corrections were required to offset the effect of a rising versus falling hydrograph and the wake produced by the presence of the sensor in the flow. Table 2 lists the range of values and associated error for the measurement devices used.

Table 2 Flow Rate and Water Depth Measurement Error

Measurement	Max. Value		Error	
Inflow Rate	3.03	liters/s	± 0.02	liters/s
Outflow Rate	3.03	liters/s	± 5.0	percent
Simulator Flow Rate	4.00	mm/min	± 2.0	percent
Water Depth	30.0	mm	± 1.0	mm
Bed Slope	0.0032	m/m	± 0.0002	m/m

Velocity Profile and Bed Resistance. Typical flow depths in the model border are less than 20 mm and have Froude numbers ($V/\sqrt{gd}$) less than 0.45. The gravel used in the flume has a mean spherical equivalent diameter of 13.6 mm and a drainable porosity of 41%. Because of the small ratio of flow depth to bed material diameter, it is critical that the correct bed reference point be used in calculating normal flow depth. The longitudinal flow profile was determined to be uniform in the middle 36.6 meters of the 61 meter model border for steady state, no infiltration conditions.

However, at every partition separating each infiltration simulator a localized decrease in flow depth was measured. The source of this disturbance is assumed to be explained by the partitions preventing any flow through the gravel bed, and thus the partitions act as a constriction. Figure 13 illustrates this problem. The purpose of the partitions is to restrict flow in the gravel bed between partitions, thus it is difficult to avoid this distrubance. However, since the driving potential for flow through the gravel is primarily the difference in bed elevation between each partition (13 mm), the magnitude of the distrurbance should decrease with a decrease in bed slope. Nonetheless, the question still exists as to whether the steady flow is uniform because of this disturbance.

Figure 14 shows a velocity profile for the gravel bed. Integration of the velocity curve in Figure 14 results in Figure 15 which is a plot of cumulative flow rate per unit width versus depth. The bed reference point was taken as the depth in which 95% of the total flow passes above. This point is illustrated by a dashed line in Figure 15.

The velocity profile shown in Figure 14 was measured at a 2.6 liters/second flow rate and a zero infiltration rate. The profile was measured at the center line of the traverse at a longitudinal location 1 meter downstream of a partition, and 17.1 meters from the inlet of the model border. A 3 mm diameter pitot tube and a micromanometer were used to measure the velocity head.

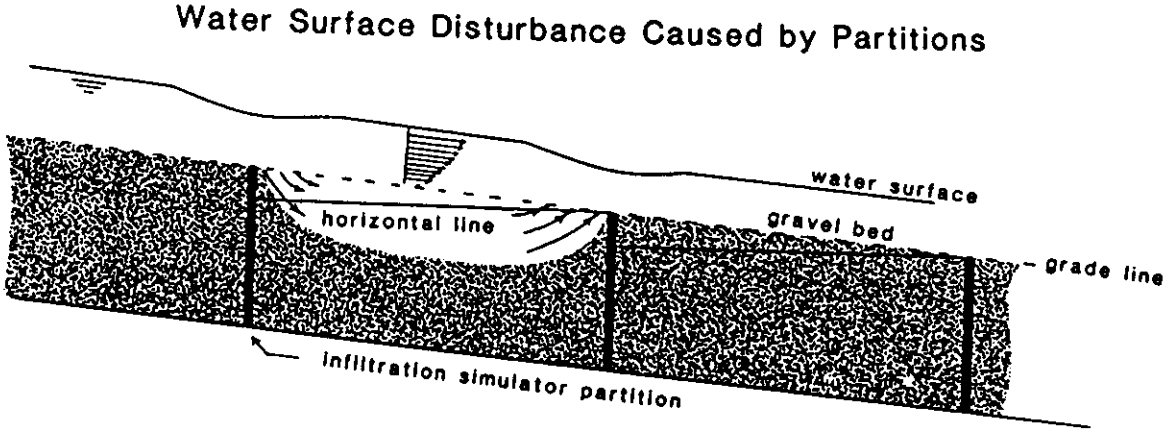

Figure 13 Water Surface Distrurbance Caused by Partitions

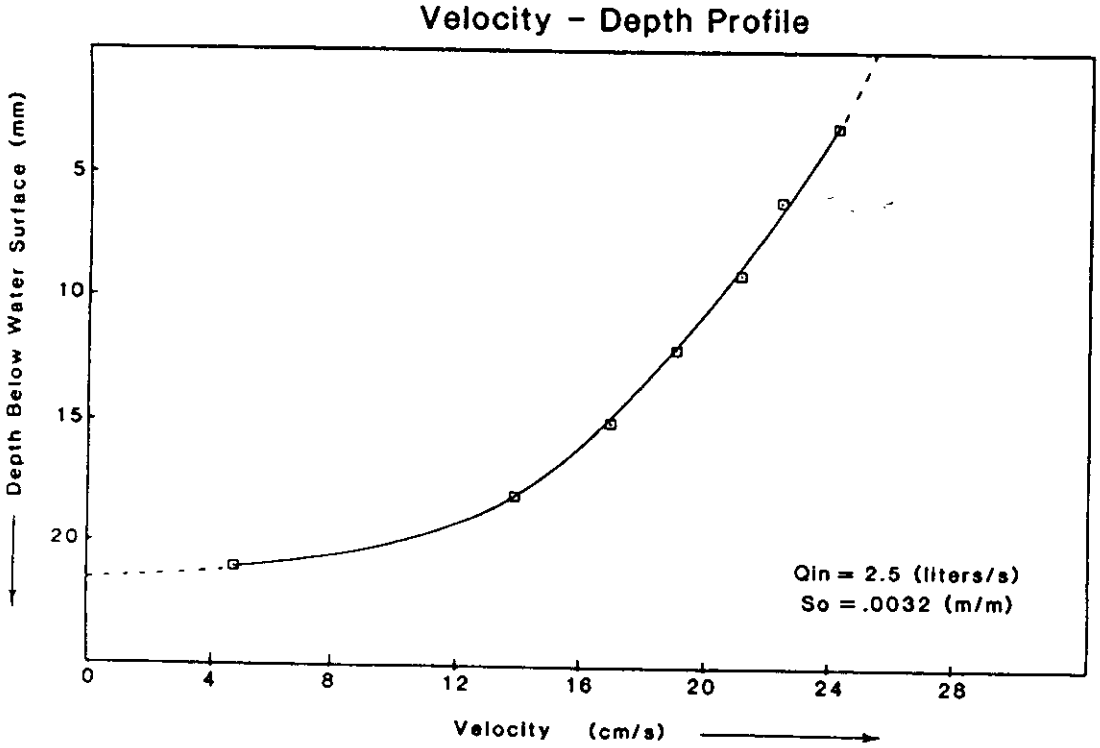

Figure 14 Velocity Profile

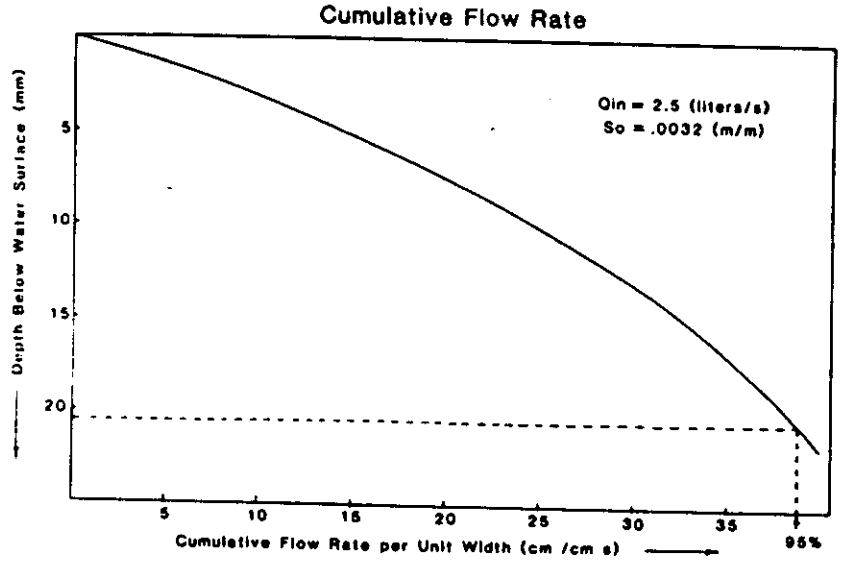

Figure 15 Cumulative Flow Rate per Width versus Depth

Ideally, the velocity profile should have been measured for several flow rates (flow depths) and several unique bed reference points calculated. However, because the velocity heads were rather small (typically less than 2 mm) and thus difficult to measure, only one profile was measured. All other velocity profiles were assumed to be of similar shape and only differ in magnitude. Once the bed reference point was established for several flow rates, and assuming uniform flow, the calculation of Manning's η is straight forward. Table 3 list the flow rates, flow depths, and Manning's η for a range of flows possible in the model border. Figure 16 shows a plot of Manning's η verses flow rate.

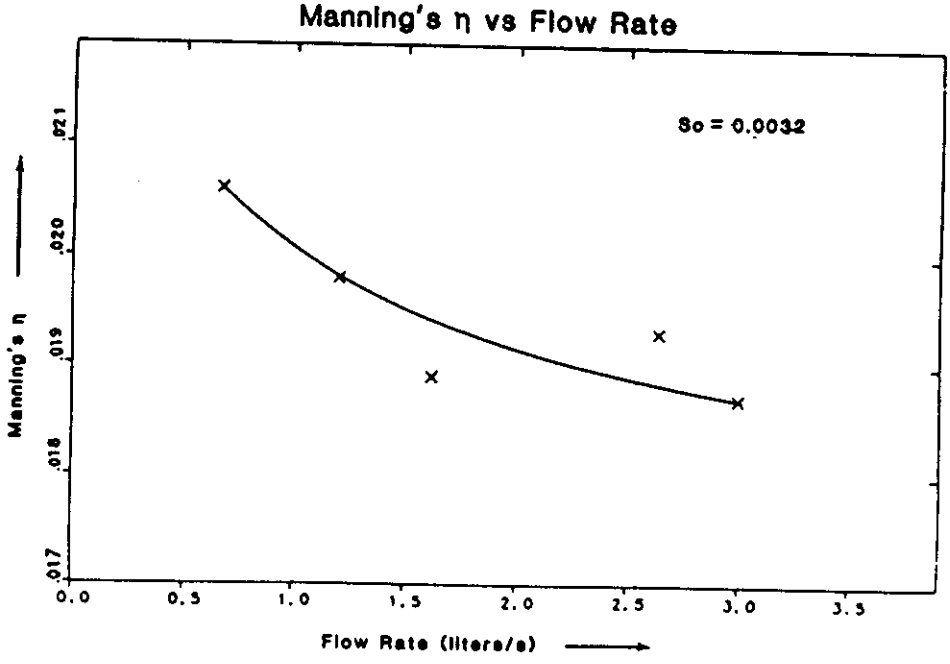

Figure 16 Manning's η versus Flow Rate for Model Border

Table 3 Flow Rate, Flow Depth, and Manning's n

Flow Rate (liters/s)	Flow Depth (mm)	Manning's n
0.67	7.9	.0206
1.20	11.0	.0198
1.62	12.8	.0189
2.64	17.4	.0193
3.00	18.4	.0187

Note that the flow depth in Figure 15 is approximately 21 mm and the flow rate is 2.5 liters/second. Interpolation of the values in Table 3 indicate that the depth of flow is less than 17.4 mm for a flow rate of 2.5 liters. This discrepancy between Figure 15 and Table 3 is because the values in Table 3 are averages of many measurements at different locations in the physical model, whereas Figure 15 is from measurements at a single location.

Uniqueness of Physical Model. The physical model of an irrigation border, described in this paper, is the first known model which can simulate a dynamic infiltration function such as may occur during surge flow irrigation. The model border is also over three times as long as any known previous precision model used for irrigation hydrodynamics research. Because the model is fully automated, many experiments can be performed with only a small amount of labor. The results will undoubtedly be useful in evaluating the accuracy of several numerical models of free surface flow with an infiltrating bed, and in developing design criteria for efficient surge flow irrigation systems. Results of early tests with the model are presented in the **Principle Findings** section of this Report. More advanced tests will be conducted as part of a follow up research project.

Field Infiltration Tests.

Accurate determination of infiltration parameters is a critical necessity for the design and operation of efficient furrow irrigation systems. The complexity of the physical processes which govern infiltration in furrows, and the nonhomgeneous, anisotropic conditions which often exist in irrigated fields have prevented the development of infiltration theory which can accurately predict infiltration rates based on soil parameters. Therefore, the practicing irrigation engineer generally continues to depend on direct measurement of infiltration using infiltrometers or rate-of-advance (volume balance) methods.

Rate-of-advance methods use advance, inflow, and outflow data collected during an irrigation event to determine the average infiltration parameters. Elliott and Eisenhauer (1983) outline the details to several rate-of-advance methods for continous flow irrigation. Latorte (1985) outline a rate-of-advance technique for estimating infiltration and surface storage for surge flow irrigation. The infiltration parameters determined from these methods are representative of the entire furrow length, which is a significant advantage when compared to infiltrometer methods. However, none of the current rate-of-advance methods account for the effect of wetted perimeter on infiltration.

Infiltrometer tests have been used for several decades and have the advantage over rate-of-advance methods of being easy to perform and requiring simpler data analysis methods, and are capable of controlling the wetted perimeter in the furrow test section. Blocked furrow infiltrometers have been used for many years to estimate the infiltration in furrows. Recently, use of the recirculating infiltrometer has become popular. Both blocked and recirculating furrow infiltrometer tests were performed during the course of this research. The following sections outline the procedures used in these tests.

Blocked Furrow Infiltrometer. Determination of infiltration from infiltrometer data is based on conservation of volume. The time rate of change of the volume of water in the infiltrometer is measured during the infiltration test. Application of conservation of volume to continuous flow recirculating or static blocked furrow tests is straight forward, and assumes that the time rate of change of volume in the infiltrometer reservoir is proportional to the infiltration rate. Infiltration during continuous flow or static tests can be described by the as

$$\frac{dS_r}{d\tau} = c\,\frac{dZ}{d\tau} \qquad (34)$$

where S_r is the volume of storage in the infiltrometer reservoir, c is a constant of proportionality, and Z is cumulative infiltrated volume per unit length of the furrow test section.

Recirulating Furrow Infiltrometer. A typical schematic of a recirculating furrow infiltrometer is shown in Figure 17. Application of conservation of volume to recirculting furrow infiltrometers is more complex for surge flow tests than for continuous or static flow tests. Figure 18 shows the net pumped volume of water during a surge flow recirculating infiltrometer test. The net pumped volume is the measured volume of water pumped out of the infiltrometer reservoir and into the upstream sump, minus the volume pumped into the resevoir from the downstream sump. Determination of infiltration from the net pumped volume requires the analysis of surface storage of water in the furrow, and the volume of water infiltrating during the advance and recession stages of the surge flow. The total amount of water stored on the surface of the soil consists of drainable storage and depression storage.

A critical point in analyzing recirculating infiltrometer data is to be sure to account for residual infiltration that occurs during the time after flow stops and before the furrow surface storage disappears. Depression storage is a factor that must be included in this analysis. If these factors are not properly accounted for, the measured furrow infiltration could be considerably less than that which actually occurs.

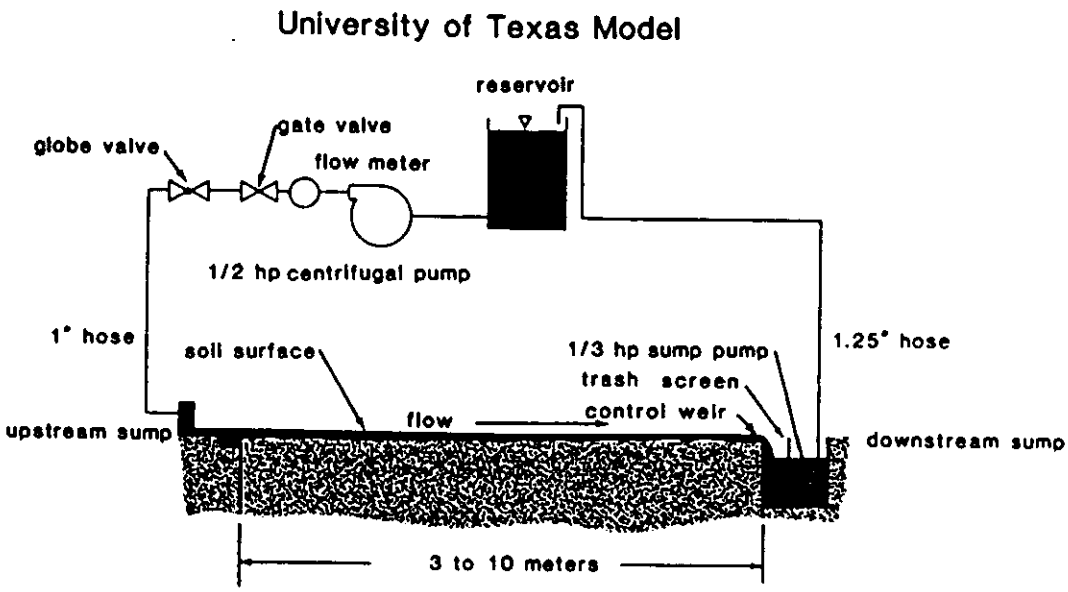

Figure 17 Schematic of a Recirculating Furrow Infiltrometer

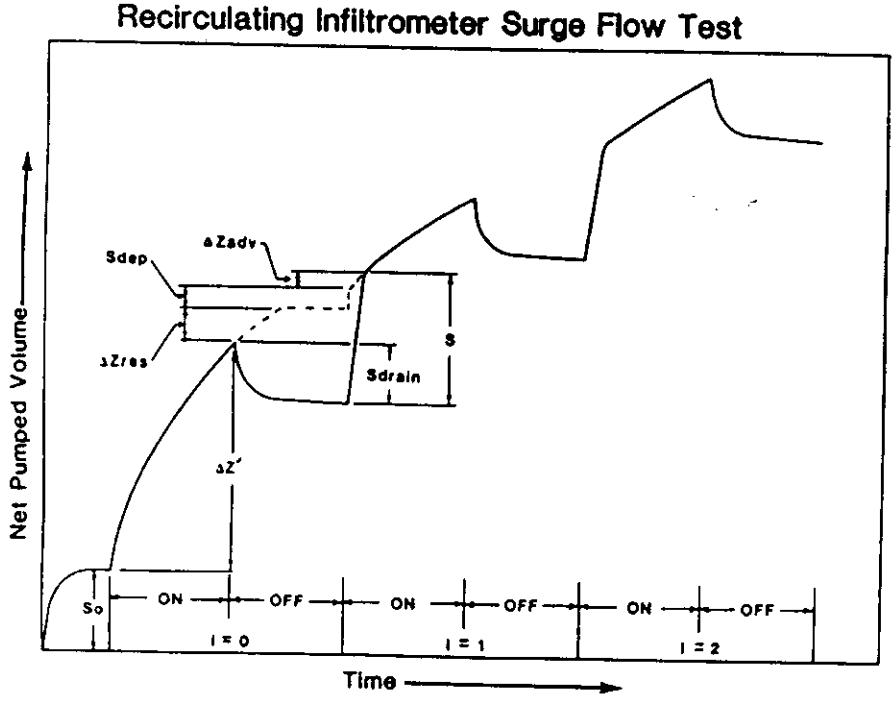

Figure 18 Surge Flow Recirculating Infiltrometer Test Data

Table 4 Calculated and Measured Infiltration and Storage Parameters

Parameter	Defined as
S_o	Total surface storage and measured as the volume of water pumped into the furrow test section which is temporarily covered with plastic.
S_i	The measure amount of water pumped into the infiltometer at the beginning of a new surge period.
$S_{drain,i}$	The measured amount of water drained and pump backed into the reservoir end of the ith surge.
$S_{dep,i}$	The calculated amount of water stored in surface depression in the furrow test section.
$\Delta Z_{adv,i}$	The calculated amount of water which infiltrates during advance and stabilization period at the beginning of the second (i=1) and every subsequent surge flow period.
$\Delta Z_{res,i}$	The calculated amount of water which infiltrates during the recession and drainage period at the end of every surge flow period minus S_{dep}.
ΔZ_i	The calculated amount of water which infiltrated during ith surge flow period.
$\Delta Z_i'$	The measured amount of water which infiltrated during ith surge flow period (see Figure 18).

Application of conservation of volume can be used to determine the cumulative infiltration curve from the net pumped volume curve shown in Figure 18. The following equations are used to do such:

$$Z_n = \sum_{i=0}^{n} \Delta Z_i \tag{35}$$

$$\Delta Z_i = \Delta Z_i' + \Delta Z_{adv,i} + \Delta Z_{res,i} + S_{dep,i} - S_{drain,i} \tag{36}$$

where $\Delta Z_{adv,o} = 0$

$$S_{dep,i} = S_o - S_{drain,i} \tag{37}$$

$$\Delta Z_{res,i} = S_i - S_{dep,i} - \Delta Z_{adv,i+1} \tag{38}$$

The value of $\Delta Z_{adv,i}$ is determined by extrapolation of a curve fit to the data collected just after advance is complete and prior to the next OFF period. Figure 18 indicates $\Delta Z_{adv,i}$ by a dotted line which begins at the first of the ON period. The values of ΔZ_i, $S_{drain,i}$ and S_i are obtained from the infiltrometer data.

Total surface storage is assumed to be equal to **S** which is measured by covering the furrow test section soil surface with a plastic liner and recirculating water through the furrow. This assumption is only valid if the plastic liner fully conforms to the furrow bed, the furrow does not change shape or erode during the test, and depth of flow with the liner in place is identical to that with the liner removed. All three of these assumptions are violated to a some degree during every test. Total surface storage can also be calculated from furrow profile measurements and either wetted perimeter, top width of the water surface, or depth of flow measurements. Perhaps the most appropriate method for detemining total surface storage would consist of measuring the furrow profile and wetted perimeter prior to each surge period.

F. PRINCIPLE FINDINGS

This research addressed three major factors which are critical to the proper design and operation of surge flow furrow irrigation systems: a) development of a surge flow furrow infiltration model; b) evaluation of the effect of wetted perimeter on infiltration in furrows; and c) the development of a numerical model of surge flow furrow irrigation which can be used to determine the optimal cycle ratio and time using site specific parameters. The findings from this project resulted in an improved methodology to analyze surge flow systems. Currently, a continuing surge flow research effort is being undertaken which will further refine this methodology and expand the amount of surge flow field and laboratory data available for analysis.

F.1 Results from Infiltrometers Tests

Evaluation of Surge Flow Infiltration Models. The cycle ratio-time and step function models, outlined in the **Methodology** section of this report, was developed as part of this project. It and the step function model were evaluated using field infiltration data collected with a recirculating furrow infiltrometer.

Continuous Flow Infiltation Coefficients. Both the cycle ratio-time infiltration model and step function model are based on empirical coefficients for continuous flow infiltration equations. The model coefficients, **k**, **a**, and **b** in equation (2) were determined from several continuous recirculating furrow infiltrometer (RFI) tests for different wetted perimeters. The coefficients $\tilde{k}$, $\tilde{a}$, and $\tilde{c}$ in equation (32) and (33), were were determined using a continuous RFI test at a wetted perimeter approximately

equal to the average wetted perimeter of all the surge flow RFI tests. The nonlinear term coefficients, $\tilde{k}$ and $\tilde{a}$, were determined from the first 90 minutes of the test period, and the linear term coefficient, $\tilde{c}$, was determined from the last 270 minutes of the infiltration test.

Predicted and Observed Cumulative Infiltration. The cycle ratio-time model was initially (Blair, Smerdon, and Rutledge 1984) evaluated using available surge infiltrometer data obtained from Malano (1980). However, these data only included a cycle ratio of $r = 0.50$ and cycle time of $t_c = 30$ minutes. Additional data with a range of r and t_c were obtained. The data herein evaluated include r values of 0.25, 0.33, 0.50 and 0.75, and t_c values of 60, 90 and 120 minutes. This provided an opportunity to test the effect of r and t_c on infiltration.

The infiltration models were evaluated using relative difference error representation defined by

$$\text{Relative Difference} = \frac{Z_{t_c,r,i,obs} - Z_{t_c,r,i,pred}}{Z_{t_c,r,i,obs}} \qquad (39)$$

where **obs** is an observed (measured) value, and **pred** is a value predicted by an intake model. Table 5 gives the relative difference for the six surge flow tests performed. Overall, there is little difference between the two models, but the cycle ratio-time model appears to predict the surge flow infiltration slightly more accurately than the step function model (the hypothesis that the cycle ratio-time model is more accurate than the step function model has a 75% probability of acceptance). However, these data are not sufficient to state that the model is clearly superior. Figure 19 shows representative field data for continuous and cycle ratio tests.

Table 5 Relative Difference in Cumulative Infiltration for Surge Flow

t_c	r	Cycle*	Cumulative On Time	Relative Difference Surge Flow Intake Model	
				Cycle Ratio-Time	Step Function
60	.75	1	90 minutes	.03	.12
60	.50	1	60	.17	.25
60	.50	2	90	-.20	-.09
60	.25	1	30	.12	.20
60	.25	2	45	.16	.24
60	.25	3	60	.11	.18
60	.25	4	75	.07	.13
60	.25	5	90	.10	.05
90	.33	1	60	.09	.04
90	.33	2	90	.05	-.01
120	.50	1	60	.08	.05

*Cycle is 0 for the first surge, cycle is 1 for the second, etc.

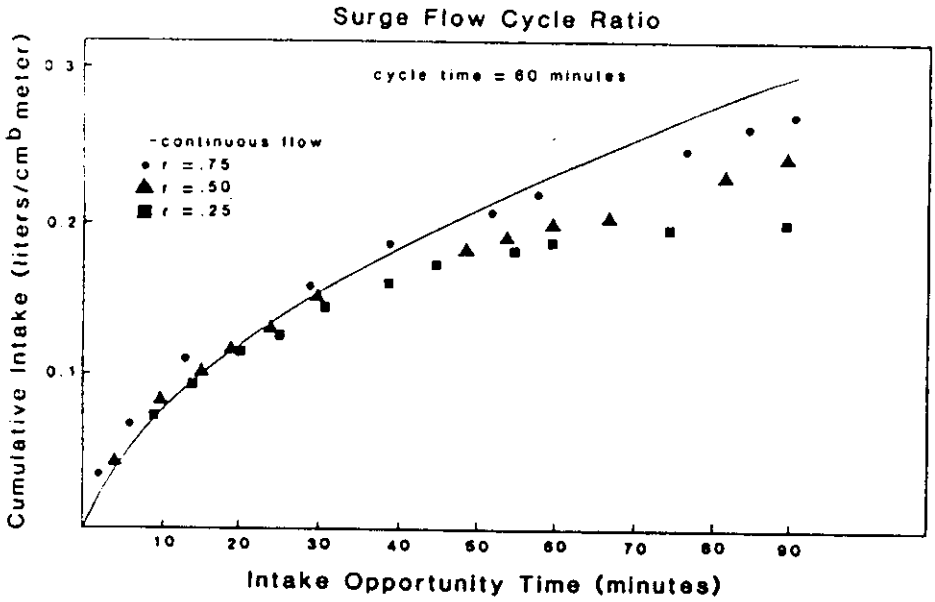

Figure 19 Recirculating Infiltrometer Tests with Cycle Ratios of 0.25, 0.50, and 0.75.

Figure 19 shows that cycle ratio is important in determining the degree of modification in the infiltration which results from surge flow. Further, this modification is in the direction which is predicted by the cycle ratio-time surge infiltration model. This supports the general applicability of such a model in surge flow irrigation analysis.

The previous evaluation of the cycle time-ratio model (Blair, Smerdon, and Rutledge 1984) using published data (Malano 1980) showed that the model accounted for 78% of the reduction in infiltration which occurs during surge flow. It is not clear if the Malano's data considered the residual intake during the OFF period. However, if it did not, the accuracy of the model would be greater than previously reported.

The results listed in Table 5 indicate that the two models tend to under predict cumulative intake. The cycle ratio-time model requires two empirical coefficients (**k** and **a**) versus the three coefficients ($\tilde{k}$, $\tilde{a}$, and $\tilde{c}$) required by the step function model. Because the step function model is not a function of cycle ratio, the accuracy of this model could be affected by the selected cycle ratio.

Because of the limited amount of data, the results are not considered conclusive, and may be specific to the sandy loam field in which the tests were performed. Both models were evaluated using constant wetted perimeter flow conditions which are produced by the recirculating furrow infiltrometer. During an actual surge irrigation, there exists a portion of the furrow which is wetted during the off time when water is advancing. This section of the furrow has a much smaller wetted perimeter than the rest of the upsteam furrow, and must be accounted for when calculating intake

during the next cycle period. The data support the concept of a simple cycle ratio-time model derived on the assumption that the physical processes within the soil which reduce infiltration with time continue unabated after being initiated. Although we recognize that other factors such as sediment sealing of the soil surface are involved, the cycle ratio-time model is based on processes (clay hydration and reduction of hydraulic gradient) known to occur in the soil during infiltration. Moreover, it is simple and, based on the data available, appears to be reasonably accurate. Finally, it can be used to estimate surge infiltration for difference values of r and t_c if continuous flow infiltration coefficients are available.

Effect of Wetted Perimeter on Infiltration in Furrows. Most previous design methods for surface irrigation systems were based on methods derived for irrigation borders. Because of this, little or no emphasis was placed on the effect of furrow geometer (i.e. wetted perimeter) on infiltration. However, field data collected as a result of this project indicate that the wetted perimeter strongly affects infiltration in furrows during the initial wetting period, and ignoring this effect would result in a significant error. Therefore, one effort of this project was to develop an empirical infiltration model which describes this effect.

Infiltration data were collected during the summer of 1984 in a sandy loam field in Safford, Arizona. The field had been in winter barley and prior to the testing had been disked and furrowed. Very little rain had fallen between harvest of the barley and the test date, and the top 24" of soil profile were very dry.

A blocked furrow infiltrometer was used to measure infiltration for various values of wetted perimeter. The wetted perimeter was held constant during each test. The infiltrometer consisted of a 55 gallon reservoir, two sheet metal plates, hoses, and a float valve. Initially the furrow test section was lined with plastic and then filled with water. At the beginning of the test the lining was removed and the water level in the reservoir was recorded every 10 minutes.

The furrow test cross sections were profiled before and after the infiltration tests. The furrow shape coefficients, defined in equation (3), for each test are listed in Table 6. The furrow ridges were less pronounced after the test than before, which is indicated by a reduction in the μ_z coefficient. The coefficients for all four blocked furrow tests were similar.

The wetted perimeter was both measured and calculated based on flow depth and surface storage. The surface storage was determined by measuring the amount of water ponded in the test section with a plastic liner covering the soil surface. The wetted perimeter was calculated using the before test furrow shape coefficients and equation (4). The relationship between top width and storage can be derived from equation (3). The flow depth was measured using a point gauge and then wetted perimeter was calculated using the after test shape coefficients. The average wetted perimeter was determined by measurements at five equally spaced intervals within the test section. All three methods produced similar values for wetted perimeter as summarized in Table 7. The variable h_o in Table 7 is defined as the maximum depth of water in a furrow cross section defined by Figure 2.

Table 6 Furrow Power Function Coefficients

Test	Length (m)	Wetted Perimeter (cm)	Furrow Shape Coefficients Prior to Test μ_1 (cm^{μ_2})	μ_2	After Test μ_1 (cm^{μ_2})	μ_2
1	1.13	28	.096	1.55	.154	1.42
2	1.02	33	.074	1.55	.115	1.44
3	1.02	37	.085	1.53	.168	1.41
4	0.99	49	.060	1.66	.098	1.53

Table 7 Calculated and Measured Wetted Perimeter Values

Test	Measured W.P. P (cm)	Measured Depth h_o (cm)	Measured Storage (cm^2)	Calculated by Storage P (cm)	Calculated by Storage B (cm)	Calculated by Depth P (cm)	Calculated by Depth B (cm)
1	28	4.5	55	24	23	26	24
2	33	5.5	98	33	31	34	32
3	37	6.0	118	35	32	35	32
4	49	9.0	230	45	41	45	41

Predicted and Observed Cumulative Infiltration. Equation (2) was evaluated using average absolute deviation (AAD), root mean square (RMS) adjusted for degrees of freedom, and r^2 coefficent as accuracy criteria. AAD, RMS, and r^2 were calculated using differences between predicted and observed cumulative infiltration.

Table 8 lists AAD, RMS, and r^2 for the equation (2). For all data sets (tests 1 through 4) the number of data points was equal to 12, and for j = 1, 2, 3...12, and the corresponding infiltration opportunity times equaled 10 ,20 ,30...120 minutes. The constant value for the number of data points and identical opportunity times were used to avoid introducing a bias between data sets. Figure 20 shows the infiltration data and the resulting infiltration curves produced from equation (2).

Table 8 Deviation between Predicted and Observed Cumulative Infiltration

Equation	Average Absolute* Deviation	Root Mean* Square Deviation	r^2 Coefficient
$Z = k\ t^a\ p^b$	2.8	3.9	0.96

* liters per meter of furrow length

Only four infiltration tests were used to evaluate equation (2), thus the results can not be considered conclusive. Also, the values of the coefficients **k**, **a**, and **b** are specific to the field in which the tests were performed. Overall, equation (2) seems to adequately describe the effect of wetted perimeter on cumulative infiltration in furrows. Furthermore, equation (2) allows this effect to range from none (**b=0**), to linear (**b=1**), or greater (**b>1**). Additional research is needed to investigate whether b can be related to furrow geometery and/or soil characteristics.

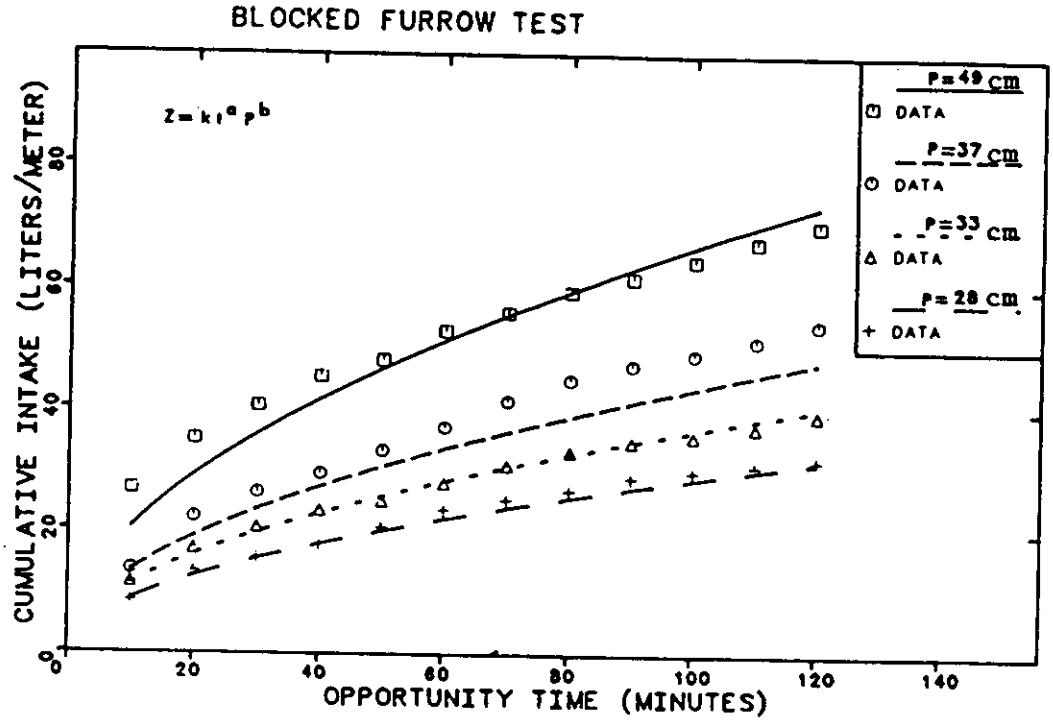

Figure 20 Effect of Wetted Perimeter on Infiltration in Furrows

F.2 Results from Kinematic Wave Model Study

The kinematic wave and cycle ratio-time surge flow furrow irrigation model, derived in this report, can be used to determine optimal values for the cycle ratio, cycle time, number of surges, and inflow rate for a specific irrigated field. Section E.3 and Table 9 in this report list the input variables for the kinematic wave model. All of these input variables except the infiltration parameters and Manning's roughness coefficient can be accurately measured. The roughness coefficient (η) is usually estimated by inspection. The infiltration parameters (**k**, **a**, and **b**) are best determined using a recirculating furrow infiltrometer. Strelkoff and Clemmens (1984) remark that "the accuracy of the (numerical) solutions outweights current ability to specify the input parameters"; and "the best defense against uncertainties ... consists of developing a likely range of variation ... so to get a range of output rather than a single figure." Therefore, η, **k**, **a**, and **b** are the variables for which a range of solutions should be modeled.

Figure 21 illustrates the distribution efficiency (Christansen's uniformity coefficient) versus the value of the infiltration equation exponent a for a hypothetical irrigated field. In Figure 21 the distribution efficiency for continuous flow infiltration is dipicted by the dashed line extending to the left of each curve. Table 9 lists the values of the computer input variables. Only the values of a and t_c were varied. All other variables were held constant. Figure 21 shows that efficiency is strongly influenced by the exponent a, and that the optimal value of t_c has a flat solution region. Furthermore, in this example the increase in efficiency of surge flow over continuous flow for a = 0.50 and a= 0.55 is relatively small. Note that the distribution efficiency for continuous is already in the vicinity of 90%. However, for a = 0.60 and a = 0.65 significant improvement in efficiency is possible. Also, at small values of t_c, surge flow efficiency can be lower than that of continuous flow.

The variation of efficiency with t_c has two limits: first, as $t_c \rightarrow 0$ the flow from subsequent surges will merge and surge flow will act like continuous flow with Q_{in} decrease proportional to the cycle ratio r; secondly, when t_c is greater than the time it takes for water to reach the end of the furrow, surge flow distribution efficiency should be identical to continuous flow efficiency.

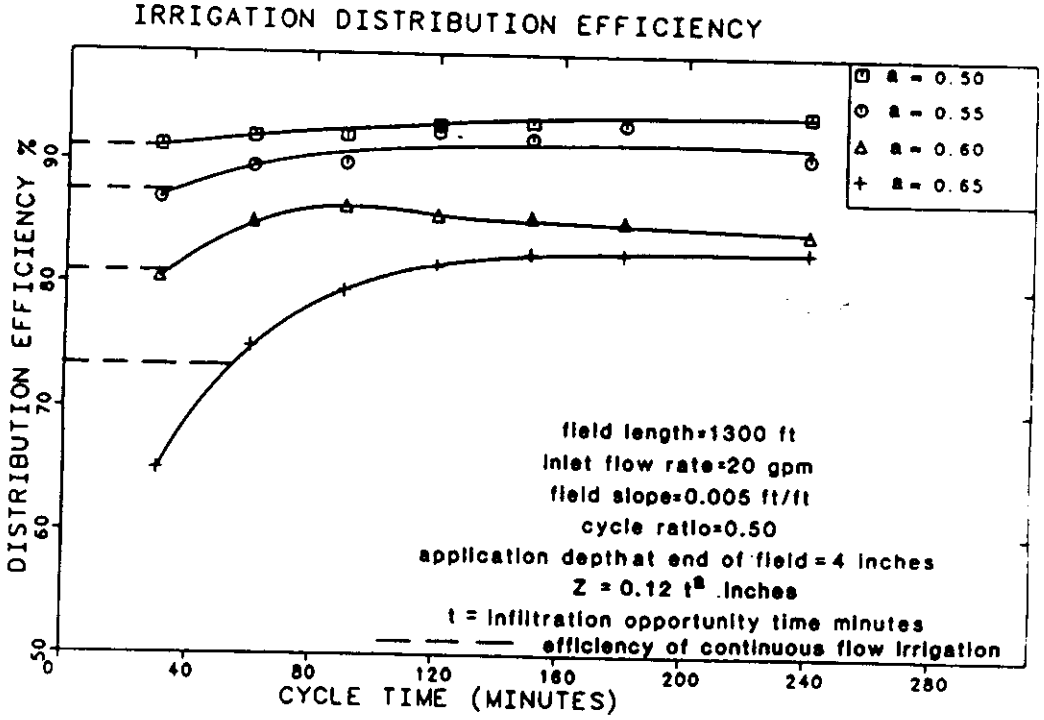

Figure 21 Irrigation Distribution Efficiency versus Cycle Time

Table 9 Hypothetical Irrigated Field Computer Model Input Data

Variable	Value
Furrow Spacing	40 inches
Furrow Length L	1300 feet
Longitudinal Slope S_b	0.005 ft/ft
Furrow Shape Parameter μ_1	0.65 ft/ft^{μ_2}
Furrow Shape Parameter μ_2	1.75 -----
Desired Application Depth at End of Field d	4 inches
Inlet Flow Rate Q_{in}	20 gpm
Infiltration Equation Exponent a	variable
Infiltration Equation Coefficient k	0.12 inches[a]
Infiltration Equation Exponent b	0 -----
Surge Flow Cycle Ratio r	0.50 -----
Surge Flow Cycle Time t_c	variable
Manning's Roughness Coefficient n	0.035 $s/ft^{1/3}$

F.3 Performance of Physical Model

The performance of the model border was evaluated using a continuous flow, constant infiltration rate test, and comparing the model border results with these numerical solutions models. All variables which are inputs to the numerical models were accurately measured in the physical model. Figure 22 indicates that advance rate for the numerical models and the model border are almost identical. Currently, the model border is being used to simulate surge flow irrigation, and a continuing research project will report on the results. The curve labels in Figure 22 define the results from the physical model border (BORDER), the hydrodynamic numerical model (HD), the zero inertia numerical mode (ZI), and the kinematic wave numerical model (KW).

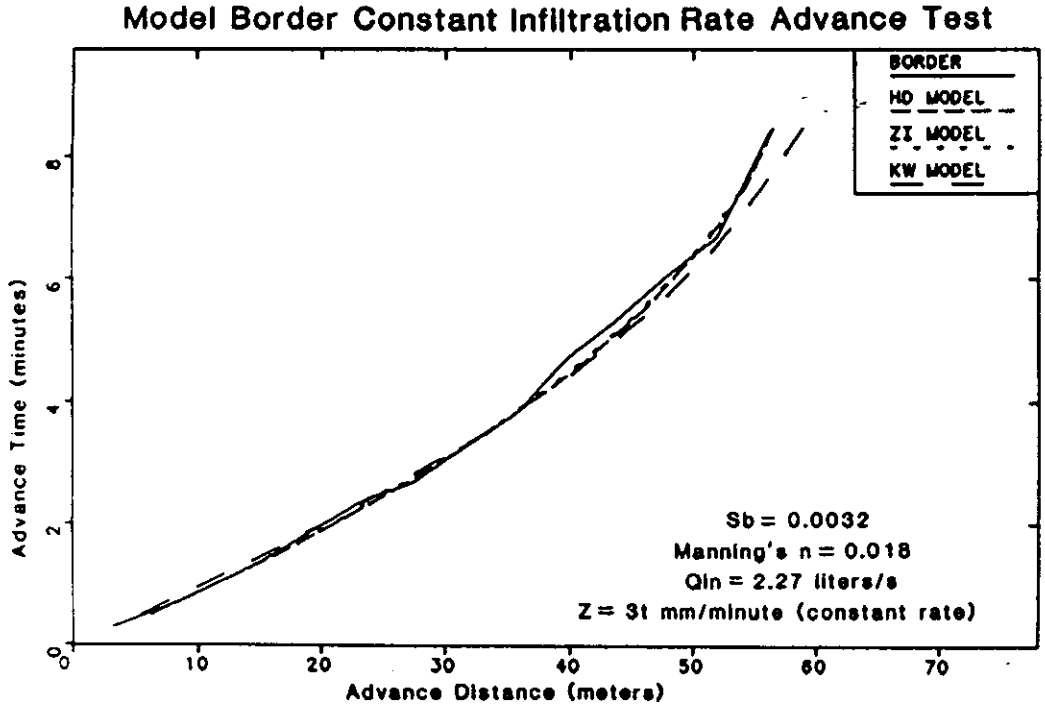

Figure 22 Observed versus Predicted Advance in the Model Border

G. CONCLUSIONS AND RECOMMENDATIONS

This research investigated the basic infiltration and hydrodynamic relationships which govern surge flow irrigation and how these relationships effect irrigation efficiency. The majority of irrigation engineers agree that infiltration is the dominate physical system which controls surface irrigation efficiency. And that the improvement of surge flow over continuous flow irrigation is due to the effective reduction in infiltration brought about by surge flow. This research supports the hypothesis that the hydration of clay particles in the soil, and the reduction of the hydraulic gradient within the soil profile are chiefly responsible for the effective reduction in infiltration due to surge flow. Futhermore, the important effect of wetted perimeter on infiltration in furrows was demonstrated. It should be noted that the effect of wetted perimeter has been ignored in almost all previous research.

Because infiltration is a function of a hydraulic parameter (wetted perimeter) it must be treated as a dependent variable in the solution of the continuity and momentum equations which describe surge flow hydrodynamics. Again, it is common practice to treat infiltration as independent from the hydraulics parameters. The resulting error caused by ignoring the effect of wetted perimeter on infiltration may be significant in many cases.

Five specific conclusions from this research are:

1) The effective reduction in infiltration as a result of surge flow can be accurately modeled using an empirical infiltration equation and assuming that the physical processes within the soil, which reduce infiltration with time, continue unabated after the soil is first wetted.

2) The effect of wetted perimeter on infiltration can be significant. Thus, infiltration must be treated as a dependent variable in the solution of the continuity and momentum equations describing surge flow irrigation.

3) Ignoring the surface storage of water within the furrow test section during a surge flow recirculating furrow infiltrometer test can result in significantly under estimating the total amount of infiltrated water, and over estimating the amount that surge flow reduces infiltration. Also, this error accumulates with each surge period. Therefore, even if the error is small during any individual period, the overall error may still be significant.

4) Hypothetical surge flow irrigation simulations indicate that for many high intake rate soils, surge flow has the potential for markedly improving distribution efficiency. However, the simulations also indicated that the potential exists for surge flow to have a lower efficiency than conventional continuous irrigation. Furthermore, the effictiveness of surge flow is highly dependent on the soil infiltration characteristics and little improvement in distribution efficiency is expected from low intake rate soils.

5) A computer controlled 200 ft long model border/furrow was designed, built and calibrated. Results indicate that this physical model of a surface irrigation system can accurately simulate field conditions for a large range of soil infiltration characteristics. Continuing surge flow research will use this model to verify numerical models of surge flow. It can also be used to determine the sensitivity of models to hydraulic roughness in the model border/furrow.

Surge flow hydrodynamic and infiltration research was initiated only a few years ago, and only a limited amount of research concerning the basic phenomena of surge flow irrigation has been performed. A noticable lacking of research into the soil physics of surge flow exists in current literature, and it is extremely necessary that future efforts incorporate research from this field. However, surge flow irrigation is currently practiced in the High Plains region of Texas, and thus an immediate need exists for simple and effective design methods. The computer model presented in this report is a beginning to the fulfillment of this need. But, additional refinement of this model and simplification of the results to a design manual are highly desirable. A continuing effort will be undertaken to meet this need in an subsequent project which is partially funded by the USGS.

Additional recirculating infiltrometer tests, conducted on a wide variety of irrigated soils, should be performed because infiltration data is critical to good surge irrigation design. Also, such data could be used to further evaluate the adequacy of the surge flow infiltration model presented in this report. If futher research supports the validity of the model, then surge infiltration characteristics can be inferred from continuous infiltration data, an important advantage. Also, additional infiltration tests should be done to develop and refine the optimization procedures used in surge irrigation system design. This should include the effects of varying the cycle ratio and cycle time, recognizing that any optimal design must conform to the constraints of the water supply system and conditions in the field.

APPENDIX A: REFERENCES

APPENDIX A: REFERENCES

ASAE, 1980, M.E. Jensen, Editor, Design and Operation of Farm Irrigation Systems, American Society of Agricultural Engineers, St Joseph, Michigan, 829 p.

Bishop, A.A., W.R. Walker, L.N. Allen, and G.J. Poole, 1981, "Furrow Advance Rates Under Surge Flow Systems," Journal of the Irrigation and Drainage Division, ASCE, 107(IR3), p. 257-265.

Blair, A.W., 1984, "Infiltration and Surge Flow," Proceedings of the Surge Flow Flow Irrigation Conference, Midland, Texas, Texas Agricultural Extension Service, Ft. Stockton.

Blair, A.W., E.T. Smerdon, and J. Rutledge, 1984, "An Infiltration Model for Surge Flow Irrigation," Proceedings of the 1984 ASCE Irrigation and Drainage Specialty Conference, Flagstaff, Arizona, p. 691-700.

Blair, A.W., and E.T. Smerdon, 1985a,"Effect of Wetted Perimeter on Infiltration in Furrows," Proceedings of the 1985 ASCE Irrigation and Drainage Division Specialty Conference, San Antonio, Texas, p. 162-169.

Blair, A.W., and E.T. Smerdon, 1985b,"Effect of Surge Cycle Ratio and Cycle Time on Infiltration," Proceedings of the 1985 ASCE Irrigation and Drainage Division Specialty Conference, San Antonio, Texas, p. 154-161.

Blair, A.W., and E.T. Smerdon, 1985c,"Design and Calibration of a 200-ft Model Irrigation Border with a Computer Controlled Infiltrating Bed," Proceedings of the 1985 ASCE Hydraulics Division Specialty Conference, Lake Buena Vista, Florida, p. 1310-1315.

Clemmens, A.J., 1981,"Evaluation of Infiltration Measurements for Border Irrigation," Agricultrual Water Management, 3(4), p.39-46.

Coolidge, P. S., W. R. Walker, and A. A. Bishop, "Advance and Runoff Surge Flow Furrow Irrigation," Journal of the Irrigation and Drainage Division, ASCE, Vol. 108, IR1, March 1982, p. 35-42.

Cunge, J.A., F.M. Holley, Jr., A. Verwey, 1980, Practical Aspects of Computational River Hydraulics, Pitman Advanced Publishing Program, Boston, Mass., p.59-79.

Elliott, R. L. and D. E. Eisenhauer, 1983, "Volume Balance Techniques for Measuring Infiltration in Surface Irrigation," ASAE Winter Meeting Paper No. 83-2520, p. 1-21.

Elliott, R. L., W. W. Walker, and G. V. Skogerboe, "Furrow Irrigation Infiltration Parameters from Advance Rate and Zero-Inertia Theory," ASAE Summer Meering, Madison, Wisconsin, Paper No. 82-2103, 1982, 25 p.

Fangmeier, D.D., M.K. Ramsey, 1978, "Intake Characteristics of Irrigation Furrows," Transactions of the ASAE, 22(1), p. 696-699.

Irrigation Journal. 1984 Irrigation Survey, Vol.35, No. 1, 1985.

Izuno, F.T., T.H. Podmore, and H.R. Duke, 1984, "Infiltration Under Surge Flow Irrigation," ASAE Paper 84-2088, Summer Meeting, Knoxville, TN., 19 p.

Izuno, F.T. and T.H. Podmore, 1984, "Kinematic Wave Model for Surge Irrigation Research," ASAE Paper 84-2089, Summer Meeting, Knoxville, TN., 19 p.

Jobling, G.A., and A.K. Turner, 1973, "Physical Model Study of Border-Strip Irrigation", ASCE Journal of the Irrigation and Drainage Division, 99(4), p. 493-510.

Latorte, Harold, 1984, "Volume Balance Model for Continuous and Surge Flow Furrow Irrigation," Masters Thesis, Agricultural Engineering Department, Texas A&M University, College Station, Texas.

Malano, H. M., "Comparison of the Infiltration Process Under Continuous and Surge Flow," Master's Thesis, Agricultural and Irrigation Engineering Department, Utah State University, Logan, Utah, 1982, p. 34-37.

Podmore, T. H. and H. R. Duke, "Field Evaluation of Surge Flow," ASAE Summer Meeting, Madison, Wisconsin, Paper 82-2102, 1982, 15 p.

Reddell, D. L., "Modified Rate of Advance Method for an Automatic Furrow Irrigation System," ASAE Paper No. 81-2552, 1981, 13 p.

Samani, Z. A., "Infiltration Under Surge Flow," Ph.D. Dissertation, Agricultural and Irrigation Engineering Department, Utah State University, Logan, Utah, 1983, p. 102-104.

SCS, 1974, SCS National Engineering Handbook, Section 15, Chapter 4 - Border Irrigation, Soil Conservation Service, Superintendent of Documents, U.S. Government Printing Office, Stock Number 0107-00888, Washington, DC 20402.

Souza, F., "Nonlinear Hydrodynamic Model of Furrow Irrigation," Ph.D. Dissertation, University of California at Davis, 1980, p. 1-142.

Strelkoff, Theodor, 1983, "BRDFLW - A Mathematical Model of Border Irrigation," USDA ARS Water Conservation Laboratory, Phoenix, Arizona, p. 61-69. (Draft Copy)

Strelkoff, T. and F. Souza, 1984, "Modeling the Effect of Depth on Intake in Furrows," ASCE Journal of Irrigation and Drainage Division, 110(4), p. 375-387.

Strelkoff, T. and A.J. Clemmens, 1984, "Current Status of Irrigation Modeling,"Proceedings of the ASCE Irrigation and Drainage Division Specialty 1984 Specialty Conference, Flagstaff, Arizona, p. 93-103.

Walker, W. R., J. C. Henggeler, and A. A. Bishop, "Effect of Surge Flow in Level Basins," ASAE Winter Meeting, Paper 81-2555, 1981, p. 1-13.

Walker, W. R. and T. S. Lee, "Kinematic Wave Approximation of Surged Furrow Advance," ASAE Winter Meeting, Paper No. 81-2544, 1981, p. 1-25.

Walker, W. R. and A. S. Humphreys, "Kinematic Wave Furrow Irrigation Model," Journal of the Irrigation and Drainage Division, ASCE, 109(4), 1983, p. 1-25.

Walker, W.R., and A.A. Bishop, 1982, "Energy and Water Conservation with Surge Flow ," ASCE Summer Meeting, Paper No. 82-2101, 15 p.

Wessels, W.P. and T. Strelkoff, 1968, "Established Surge on an Impervious Vegetated Bed," ASCE Journal of the Irrigation and Drainage Division, 94(1), p. 1-22.

Zur, B., "The Pulsed Irrigation Principle for controlled Soil Wetting," Soil Science, Vol. 22, No. 5, November 1976, pp. 282-291.

APPENDIX B: SURGE FLOW KINEMATIC WAVE FURROW IRRIGATION MODEL (KWFIM)

APPENDIX B: SURGE FLOW KINEMATIC WAVE IRRIGATION COMPUTER PROGRAM

The computer code listed in this appendix is intended to be used as an example application of the kinematic wave and cycle ratio-time models presented in this report. The code is intended to provide a basis for applying the methods outlined in this report; it is not intended to meet all requirements necessary for the design of a surge irrigation system.

This computer code is provided and may be used with the understanding that the Center for Research in Water Resources makes no warranties concerning its accuracy, completeness, reliability, or suitability for any particular purpose. In addition, it is understood that the Center for Research in Water Resources and The University of Texas at Austin nor anyone else shall be under no liability whatsoever to any person or organization by reason of any use made either of this computer code or the explanations which accompany it.

Capabilities of KWFIM

1) Coalescence of flow is allowed (i.e. one surge can run into a previous surge).
2) The effect of wetted perimeter on infiltration is calculated.
3) Infiltration (Z) is treated as a dependent variable in the solution.
4) Recession of one or more surges can be occurring simultaneously with the advance of one or more other surges.
5) Rear end recession can occur simultaneously with front and advance for any given surge.
6) Application, distribution, and excess/deficit efficiencies are calculated.
7) The end of the furrow must be free draining.
8) A cutback or continuation phase can be simulated.
9) Variable cycle ratios and cycle times are allowed.

Computer and Input Specifications

The KWFIM computer code was developed on a CDC 170/750 computer system using the CDC FTN5 Fortran 77 compiler with all variables initialized to zero at load time. Two common compatibility problems with compilers other than FTN5 are: the code uses array variables which are indexed from zero rather than one; and, IF THEN ELSE ENDIF statements are used. Input data is obtained from a free formatted local file named OUTPUT. No interactive control is used. An experienced FORTRAN programmer will be able to modify the input, output, and capabilities to his or her specific needs.

The input variables are listed below in the sequence they should appear in the INPUT file.

Line	Variable	Description	Units
1	QIN	inflow rate	m^3/s
1	QCONT	cutback or continuation flow rate	m^3/s
2	FS	furrow spacing	m
2	FL	field length	m
2	SB	field longitudinal slope	m/m
2	U1	furrow shape coefficient	m/m^{U1}
2	U2	furrow shape coefficient	---
2	MN	Manning's roughness coefficient	$s/m^{1/3}$
3	K	infiltration coefficient eq.(3.2)	$m^3/(m\ min^A m^B)$
3	AZ	infiltration coefficient eq.(3.2)	---
3	BZ	infiltration coefficient eq.(3.2)	---
3	CZ	initial abstraction	m^3/m
4	RO	cycle ratio	---
4	DR	increment in cycle ratio	---
4	TCO	cycle time	min.
4	DTC	increment in cycle time	min.
5	DT	finite difference time step	min.
5	TI	maximum time of irrigation (total elapsed time from start to end)	min.
5	DAD	desired application depth	m

KWFIM Subroutine Descriptions

Name	Purpose
INPUT	inputs data from file INPUT
INIT	initializes all variables and calculates any constants
RECCEL	solves the momentum and continuity equations for interior cells
INFIL	calculates infiltration and swaps variables for new time
EFF	calculates irrigation efficiency

KWFIM Flow Chart

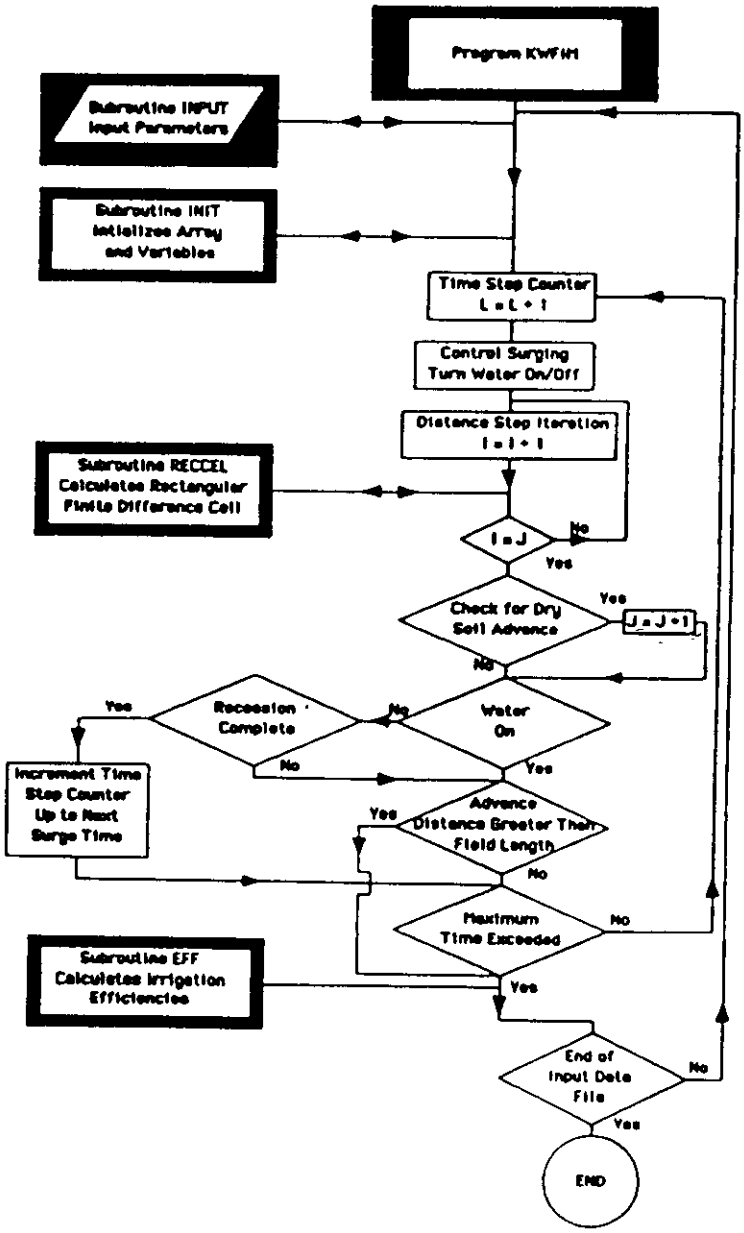

KWFIM SOURCE CODE LISTING

```
      PROGRAM KWFIM (INPUT,TTY,TAPE5=INPUT,TAPE7=OUTPUT)
C KWFIM  CRWR-BRC-UT-AUSTIN-BLAIR  CDC-FTN5  85.11.01
C
C  SURGE FLOW KINEMATIC WAVE FURROW IRRIGATION SIMULATION MODEL
C
C VARIABLE     DESCRIPTION
C QIN       INFLOW RATE (M**3/SEC)
C FL        FIELD LENGTH (M)
C SB        FIELD SLOPE (M/M)
C K,AZ,BZ      INFILTRATION COEFFICIENTS (Z=M**2)
C U1,U2       FURROW SHAPE COEFFICIENTS (M)
C MN        MANNING'S ROUGHNESS COEFFICIENT
C TC,R      CYCLE TIME (MINUTE), CYCLE RATIO
C DAD       DESIRED APPLICATION DEPTH (M)
C TI        MAXIMUM TIME OF IRRIGATION (MINUTES)
C FS        FURROW SPACING (M)
C DT        FINITE DIFFERENCE TIME STEP (MINUTES)
C NS        NUMBER OF SURGES N-O IS FIRST SURGE
C F1        FLAG USED TO TURN WATER ON OR OFF
C F2        FLAG USED TO INDICATE RECESSION IS OVER
C PSI,THETA,EPS      FINITE DIFFERENCE WEIGHTING COEFFICIENTS
C NT        MAXIMUM NUMBER OF TIME STEP
C NMAX      NUMBER OF FINITE DIFFERENCE DISTANCE GRID LINES
C AO        NORMAL FLOW AREA AT INLET TO FURROW
C ZO        INITIAL CUMULATIVE INFILTRATION
C C1-C7       FINITE DIFFERENCE CONSTANTS
C X1,X2,XL,XR,N,P1,P2 VARIABLES USED TO CALC. W1,W2,A1,A2
C A1,A2       FLOW RATE-FLOW AREA COEFFICIENTS
C W1,W2       FLOW AREA-WETTED PERIMETER COEFFICIENTS
C I         INCREMENT
C J         FINITE DIFFERENCE DISTANCE INCREMENT
C L         FINITE DIFFERENCE TIME INCREMENT
C NR        NEWTON-RAPHSON INCREMENT
C TAU       SURGE INFILTRATION OPPORTUNITY TIME (SEC)
C IAZ()       KEEPS TRACK OF ADVANCE TIMES
C A(,)      FINITE DIFFERENCE FLOW AREA (M**2)
C Z(,)      FINITE DIFFERENCE INFIL. VOLUME/LENGTH
C DX()      INCREMENTAL ADVANCE DISTANCE (M)
C XA()      CUMULATIVE ADVANCE DISTANCE (M)
C ZC()      CUMULATIVE INFIL. VOLUME/LENGTH (M**3/M)
C Y()       INFILTRATION DEPTH NONUNIFORM IN DISTANCE (M)
C
C SOURCE CODE
C
      REAL K,MN
      INTEGER F1,F2,F3,F4
C
```

```
      COMMON /A1/ IAZ(1000),A(0:1000,0:1),Z(0:1000,0:1),DX(1000),
     ;     XA(0:1000),ZC(1000),
     ;     QIN,FL,SB,K,AZ,BZ,U1,U2,MN,TC,R,CZ,
     ;     DAD,TI,FS,DT,C7,A1,A2,W1,W2,S,XZ,NS,F1,F2,PSI,THETA,EPS,NT,
     ;     MMAX,A0,Z0,TAU,J,L,A01,DT60,IFLUME,NZ,ICONT,IRECES,QCONT,DR,
     ;     DTC,TC0,R0,VRUNOF,NCONT,THETA1,PSI1,EPS1,THETA2,PSI2,EPS2
C
 10   CALL INPUT
      CALL INIT
C
C BEGIN SIMULATION
C
100   L = L + 1
      IFLAG = ICONT + IRECES
      IF(L.GT.1000) STOP
      IF(ICONT.EQ.1.AND.A(0,1).GT.A01) NCONT = NCONT + 1
      T=L*DT60
C
C TURN WATER OFF
C
      TCNR=TC*NS+TC*R
C     IF(L.GT.80) WRITE(7,*)T,TCNR,F1,IFLAG,L,NT,ICONT,IRECES,J
      IF(T.GE.TCNR.AND.F1.EQ.1.AND.IFLAG.EQ.0.AND.L.LT.NT.AND.F3.GE.NS)
     ; THEN
      WRITE(7,*)'***** ',NS,T,XA(J)
C       CALL OUTPUT (T,NS+4,2,0)
        F1=0
        A(0,0)=.01*A0
        A(0,1)=.01*A0
        PSI=PSI2
        EPS=EPS2
      ENDIF
C
C
C TURN WATER ON
C
      TCNS=TC*(NS+1)
      IF(T.GE.TCNS.AND.F1.EQ.0.AND.IFLAG.EQ.0.AND.XA(J).LT.FL)THEN
        F1=1
        NS=NS+1
        TC = TC0 + DTC*NS
        R  = R0  + DR*NS
        A(0,0)=A0
        A(0,1)=A0
        PSI=PSI1
        EPS=EPS1
      ENDIF
      DO 500 I=1,J
        TAU=(L-IAZ(I)+1)*DT60
        CALL RECCEL (I)
```

```
          IF (TAU.GT.DT60.AND.A(I,0).GT.0.AND.A(I,1).GT.0) THEN
          Z(I,1)=Z(I,0)+C7*DT60*((TAU-DT60)**(AZ-1)*A(I,0)**(W2*BZ)+
        ; TAU**(AZ-1)*A(I,1)**(W2*BZ))
          ELSE
         IF (A(I,1).GT.0)   Z(I,1)=K*TAU**AZ*(W1*A(I,1)**W2)**BZ
          ENDIF
          IF(A(I,1).GT.A01) THEN
           Z1 = (1.-EPS)*Z(I-1,0) + EPS*Z(I,0)
           Z2 = (1.-EPS)*Z(I-1,1) + EPS*Z(I,1)
           ZC(I) = ZC(I) + (Z(I-1,1)-Z(I-1,0))
          ENDIF
  500 CONTINUE
C
       IF (XA(J).GE.FL.AND.A(J,1).GT.A01)
      ; VRUNOF = VRUNOF + A1*A(J,1)**A2 * DT*1.1
C
       IF(IAZ(J+1).EQ.0.AND.A(J,1).GT.A01.AND.XA(J).LT.FL) THEN
         DX(J+1)=A(J,1)**A2*DT*THETA*A1/(PSI*A(J,1)+EPS*Z(J,1))
         IAZ(J+1)=L+1
         XA(J+1)=XA(J)+DX(J+1)
         ZC(J+1)=K*(DT60)**AZ*(W1*A(J,1)**W2)**BZ
         J=J+1
       ENDIF
       CALL INFIL
       IF(L.LT.NT.AND.F1.EQ.1) GOTO 100
       F2=0
       DO 600 I=0,J
         IF(A(I,1).GT.A01) F2 = 1
  600 CONTINUE
C
       IF(F2.EQ.0.AND.IRECES.EQ.1) GOTO 1000
       L2 = 0
       IF (F2.EQ.0) L2 = INT((NS+1)*TC/DT60)-1
       IF (F2.EQ.0.AND.IFLAG.EQ.0) L = L2
       IF(XA(J).GE.FL.AND.IFLAG.EQ.0.AND.L.EQ.L2) THEN
         ICONT = 1
         A0=(QCONT/A1)**(1/A2)
         A01 = .011*A0
         A(0,0)=A0
         A(0,1)=A0
       ENDIF
       IF(IRECES.EQ.0.AND.L.GE.NT) THEN
         IRECES = 1
         A(0,1) = 0.01*A0
         A(0,0) = 0.01*A0
         PSI = PSI2
         EPS = EPS2
       ENDIF
       GOTO 100
C
```

```
 1000 CONTINUE
      NMAX = J
      CALL EFF
C
      GOTO 10
      END
C*************************************************************************
C     INPUT DATA FROM DATA FILE: INPUT
C*************************************************************************
      SUBROUTINE INPUT
      REAL K,MN
      INTEGER F1,F2
      COMMON /A1/ IAZ(1000),A(0:1000,0:1),Z(0:1000,0:1),DX(1000),
     ;     XA(0:1000),ZC(1000),
     ;     QIN,FL,SB,K,AZ,BZ,U1,U2,MN,TC,R,CZ,
     ;     DAD,TI,FS,DT,C7,A1,A2,W1,W2,S,XZ,NS,F1,F2,PSI,THETA,EPS,NT,
     ;     NMAX,AO,ZO,TAU,J,L,AO1,DT60,IFLUME,NZ,ICONT,IRECES,QCONT,DR,
     ;     DTC,TCO,RO,VRUNOF,NCONT,THETA1,PSI1,EPS1,THETA2,PSI2,EPS2
C
      READ(5,*,END=100)QIN,QCONT
      READ(5,*)FS,FL,SB,U1,U2,MN
      READ(5,*)K,AZ,BZ,CZ
      READ(5,*)RO,DR,TCO,DTC
      READ(5,*)DT,TI,NZ,DAD,IFLUME
      READ(5,*) THETA1,PSI1,EPS1
      READ(5,*) THETA2,PSI2,EPS2
      WRITE(7,*)'U1=',U1,' U2=',U2,' MN=',MN,' TC=',TCO
      WRITE(7,*)'R=',RO,' DAD=',DAD,' TI=',TI
      WRITE(7,*)'FS=',FS,' DT=',DT
      RETURN
C
  100 STOP
      END
C*************************************************************************
C   INITIALIZE VARIABLES
C*************************************************************************
      SUBROUTINE INIT
      REAL K,MN
      INTEGER F1,F2
      COMMON /A1/ IAZ(1000),A(0:1000,0:1),Z(0:1000,0:1),DX(1000),
     ;     XA(0:1000),ZC(1000),
     ;     QIN,FL,SB,K,AZ,BZ,U1,U2,MN,TC,R,CZ,
     ;     DAD,TI,FS,DT,C7,A1,A2,W1,W2,S,XZ,NS,F1,F2,PSI,THETA,EPS,NT,
     ;     NMAX,AO,ZO,TAU,J,L,AO1,DT60,IFLUME,NZ,ICONT,IRECES,QCONT,DR,
     ;     DTC,TCO,RO,VRUNOF,NCONT,THETA1,PSI1,EPS1,THETA2,PSI2,EPS2
C
C  FP(X) FUNCTION DEFINES ARC LENGTH FORMULATE FOR WETTED PERIMETER
C
      FP(XZ)=SQRT(1.+(U1*U2)**2*XZ**(2*(U2-1)))
      DO 5 I = 0,1000
```

```
          DO 5 J = 0,1
            A(I,J)=0.
            Z(I,J)=0.
        5 CONTINUE
          DO 6 I = 1,1000
            IAZ(I)=0
            DX(I)=0.
            XA(I)=0.
            ZC(I)=0.
        6 CONTINUE
C
          L = 0
          NCONT =0
          ICONT = 0
          IRECES = 0
          VRUNOF = 0.
          TC = TC0
          R  = R0
          NS=0
          F1=1
          J=1
          IAZ(1)=1
          PSI=PSI1
          THETA=THETA1
          EPS=EPS1
          NT=TI/DT
          DT60 = DT
          DT=DT*60.
          XA(0) = 0.
C
C  CALCULATE COEFFICIENTS FOR P=W1*AREA**W2 AND Q=A1*AREA**A2
C
          X1=.1*FS
          X2=.3*FS
          N=20
C
C    INTEGRATE TO FIND WETTED PERIMETER
C
          P1=0.
          DO 100 I=1,N
          XL=X1*(I-1)/N
          XR=X1*I/N
          P1=P1+X1*(FP(XL)+FP(XR))/(2*N)
      100 CONTINUE
C
          P2=0.
          DO 200 I=1,N
          XL=X2*(I-1)/N
          XR=X2*I/N
          P2=P2+X2*(FP(XL)+FP(XR))/(2*N)
```

```
  200 CONTINUE
C
C  CALCULATE W1,W2,A1,A2 USING TWO POINT METHOD TO FIT POWER EQUATION
C
      AREA1=U1*U2/(U2+1)*X1**(U2+1)
      AREA2=U1*U2/(U2+1)*X2**(U2+1)
      W2=ALOG(P1/P2)/ALOG(AREA1/AREA2)
      W1=P1/AREA1**W2
      A1=SQRT(SB)/(MN*W1**.6667)
      A2=5./3.-2./3.*W2
      WRITE(7,*)U1,U2,X1,X2,AREA1,AREA2,P1,P2,W1,W2,A1,A2
C
      AO=(QIN/A1)**(1/A2)
      AO1 = .011*AO
      A(0,0)=AO
      A(0,1)=AO
      ZO=K*(DT60)**AZ*(W1*AO**W2)**BZ + CZ
      Z(0,1)=K*(2*DT60)**AZ*(W1*AO**W2)**BZ + CZ
      Z(0,0)=ZO
      ZC(1)=ZO
      DX(1)=THETA*A1*A(0,1)**A2*DT/(PSI*A(0,1)+EPS*ZO)
      XA(1)=DX(1)
      C7=.5*K*AZ*W1**BZ
C
      RETURN
      END
C*************************************************************************
C  CALCULATE NEW INFILTRATION AND SWAP ARRAY VALUES
C*************************************************************************
      SUBROUTINE INFIL
      REAL K,MN
      INTEGER F1,F2
      COMMON /A1/ IAZ(1000),A(0:1000,0:1),Z(0:1000,0:1),DX(1000),
     ;     XA(0:1000),ZC(1000),
     ;     QIN,FL,SB,K,AZ,BZ,U1,U2,MN,TC,R,CZ,
     ;     DAD,TI,FS,DT,C7,A1,A2,W1,W2,S,XZ,NS,F1,F2,PSI,THETA,EPS,NT,
     ;     NMAX,AO,ZO,TAU,J,L,AO1,DT60,IFLUME,NZ,ICONT,IRECES,QCONT,DR,
     ;     DTC,TCO,RO,VRUNOF,NCONT,THETA1,PSI1,EPS1,THETA2,PSI2,EPS2
      DO 100 I=0,J
C       WRITE(6,10)NS,L,I,A(I,1),Z(I,1),XA(I+1),ZC(I+1)
   10    FORMAT(10X,3I5,4F10.5)
      Z(I,0)=Z(I,1)
      A(I,0)=A(I,1)
  100 CONTINUE
      Z(0,1)=K*((L+2)*DT60)**AZ*W1**BZ*AO**(W2*BZ) + CZ
C
      RETURN
      END
```

```
C*********************************************************************
C  CALCULATE A AND Z FOR RECTANGULAR CELLS
C*********************************************************************
      SUBROUTINE RECCEL (I)
      REAL K,MN
      INTEGER F1,F2
      COMMON /A1/ IAZ(1000),A(0:1000,0:1),Z(0:1000,0:1),DX(1000),
     ;     XA(0:1000),ZC(1000),
     ;     QIN,FL,SB,K,AZ,BZ,U1,U2,MN,TC,R,CZ,
     ;     DAD,TI,FS,DT,C7,A1,A2,W1,W2,S,XZ,NS,F1,F2,PSI,THETA,EPS,NT,
     ;     NMAX,AO,ZO,TAU,J,L,AO1,DT60,IFLUME,NZ,ICONT,IRECES,QCONT,DR,
     ;     DTC,TCO,RO,VRUNOF,NCONT,THETA1,PSI1,EPS1,THETA2,PSI2,EPS2
C
      IF(A(I,0).LT.AO1) A(I,0) = .01 * AO
      IF(A(I-1,0).LT.AO1) A(I-1,0) = .01 * AO
      IF(A(I-1,1).LT.AO1) A(I-1,1) = .01 * AO
      C1=THETA*DT
      C2=PSI*DX(I)
      C3=EPS*DX(I)
      C4=((1-THETA)*A1*A(I,0)**A2-((1-THETA)*A1*A(I-1,0)**A2+THETA*A1*
     ; A(I-1,1)**A2))*DT
      C5=((1-PSI)*A(I-1,1)-((1-PSI)*A(I-1,0)+PSI*A(I,0)))*DX(I)
      C6=((1-EPS)*Z(I-1,1)-((1-EPS)*Z(I-1,0)+EPS*Z(I,0)))*DX(I)
      A(I,1)=A(I-1,1)
C
      DO 100 NR=1,5
      IF(A(I,1).LE.0)THEN
        A(I,1)=.01*AO
        RETURN
      ENDIF
      IF(TAU.EQ.DT60)THEN
        Z(I,1)=K*TAU**AZ*(W1*A(I,1)**W2)**BZ
        GO TO 90
      ENDIF
      Z(I,1)=Z(I,0)+C7*DT60*((TAU-DT60)**(AZ-1)*A(I,0)**(W2*BZ)+
     ;       TAU**(AZ-1)*A(I,1)**(W2*BZ))
   90 DZ=C7*DT60*TAU**(AZ-1)*W2*BZ*A(I,1)**(W2*BZ-1)
      F=C1*A1*A(I,1)**A2+C2*A(I,1)+C3*Z(I,1)+C4+C5+C6
      D=C1*A1*A2*A(I,1)**(A2-1)+C2+DZ
      A(I,1)=A(I,1)-F/D
  100 CONTINUE
C
      RETURN
      END
C*********************************************************************
C  CALCULATE APPLICATION, DEFICIT/EXCESS, DISTRIBUTION EFFICIENCIES
C*********************************************************************
      SUBROUTINE EFF
      REAL K,MN,Y(1000)
      INTEGER F1,F2
```

```
      COMMON /A1/ IAZ(1000),A(0:1000,0:1),Z(0:1000,0:1),DX(1000),
     ;     XA(0:1000),ZC(1000),
     ;     QIN,FL,SB,K,AZ,BZ,U1,U2,MN,TC,R,CZ,
     ;     DAD,TI,FS,DT,C7,A1,A2,W1,W2,S,XZ,NS,F1,F2,PSI,THETA,EPS,NT,
     ;     NMAX,A0,Z0,TAU,J,L,A01,DT60,IFLUME,NZ,ICONT,IRECES,QCONT,DR,
     ;     DTC,TC0,R0,VRUNOF,NCONT,THETA1,PSI1,EPS1,THETA2,PSI2,EPS2
C
      VAPP = 0.
      VDEF = 0.
      VDEEP = 0.
      DO 10 I= 0,NS
        R = R0 + DR*I
        TC = TC0 + DTC*I
        VAPP = VAPP + QIN*R*TC*60.
   10 CONTINUE
      VAPP = VAPP + NCONT*DT*QCONT
C
      DO 100 I=1,NMAX
        Y(I) = ((1.-EPS)*ZC(I)+EPS*ZC(I+1))/FS
        IF(Y(I).LT.DAD) VDEF = VDEF + (DAD-Y(I))*DX(I)*FS
        IF((Y(I)).GT.DAD) VDEEP = VDEEP + (Y(I)-DAD)*DX(I)*FS
  100 CONTINUE
      IF (XA(NMAX).LT.FL) VDEF = VDEF + DAD * FS * (FL-XA(NMAX))
      EA = (VAPP - VDEEP - VRUNOF)/VAPP
      EDE = 1. - (VDEEP+VDEF+VRUNOF)/(VAPP+VDEF)
C
      SUM = 0.
      DO 200 I = 1,NMAX
        SUM = SUM + DX(I)*Y(I)
  200 CONTINUE
      YM = SUM/FL
      SUM = 0.
      DO 300 I = 1,NMAX
        SUM = SUM + ABS((Y(I)-YM)*DX(I))
  300 CONTINUE
      IF (XA(NMAX).LT.FL) SUM = SUM + (FL-XA(NMAX))*YM
      YD = SUM/FL
      ED=(1-YD/YM)
      VERR1 = (VAPP - (DAD*FL*FS + VRUNOF + VDEEP - VDEF))/VAPP
      VERR2 = (VAPP - YM*FL*FS - VRUNOF)/VAPP
      WRITE(7,310)ED,EA,EDE
  310 FORMAT(4(/),'  DISTRIBUTION EFFICIENCY=',F10.2,
     ;/,'   APPLICATION EFFICIENCY     = ',F10.2,
     ;/,'   DEFICIT/EXCESS EFFICIENCY = ',F10.2)
C
      WRITE(7,320)VAPP,DAD2,YM,VDEEP,VDEF,VRUNOF,VERR1,VERR2
  320  FORMAT(/,'    VOLUME APPLIED      = ',F10.2,
     ; /,'    DESIRED APP. DEPTH = ',F10.4,
     ; /,'    MEAN DEPTH         = ',F10.4,
     ; /,'    DEEP PERCULATION   = ',F10.2,
```

```
     ; /,'     VOLUME OF DEFICIT  = ',F10.2,
     ; /,'     VOLUME OF RUNOFF   = ',F10.2,
     ; /,'     REL.ERROR D/E EFF. = ',F10.2,
     ; /,'     REL.ERROR DIS.EFF. = ',F10.2)
 1000 CONTINUE
      RETURN
      END
C*************************************************************************
```

APPENDIX C: NOTATION

Notation Used in This Report

Notation		Dimensions
	Physical System and Flow Process (Section E.1)	
Z	cumulative infiltrated volume per length of furrow	L^3/L
P	furrow wetted perimeter	L
$f()$	function of	-
τ	infiltration opportunity time	T
s	curvilinear distance along cross section of furrow	L
k	empirical infiltration coefficient	$L^3/(L \cdot T^a \cdot L^b)$
a	empirical infiltration exponent	dimensionless
b	empirical infiltration exponent	dimensionless
μ_1	empirical furrow shape coefficient	L/L^{μ_2}
μ_2	empirical furrow shape exponent	dimensionless
y	vertical distance (positive upward)	L
B	top width of water surface in furrow	L
x	transverse (horizontal) distance	L
r	surge flow cycle ratio	dimensionless
t_c	surge flow cycle time	T
VSP	valve sequencing pattern	-
	Kinematic Wave Model (Section E.2)	
Q_{in}	flow rate at the inlet to the furrow	L^2
P	furrow wetted perimeter	L
Z	cumulative infiltrated volume per length of furrow	L^3/L
A	flow area	L^2
Q	flow rate	L^3
$\underline{Q}$	temporal average of Q over time Δt	L^2
$\underline{A}$	spatial average of A over distance Δx	L^3
$\underline{Z}$	spatial average of Z over distance Δx	L^3/L
t	finite difference time variable	T
x	finite difference distance variable (longitudinal)	L
η	Manning's roughness coefficient	$T/L^{1/3}$
S_b	furrow longitudinal bed slope	dimensionless
S_f	slope of hydraulic grade line	dimensionless
ω_1	empirical coefficient relating A to P	$L/L^{2\omega_2}$
ω_2	empirical exponent relating A to P	dimensionless
α_1	empirical coefficient relating Q to A	$L^3/(T \cdot L^{2\omega_2})$
α_2	empirical exponent relating Q to A	dimensionless
Δt	finite difference time increment	T
Δx	finite difference distance increment	L
θ	finite difference temporal weight for Q	dimensionless
ψ	finite difference spatial weight for A	dimensionless
ε	finite difference spatial weight for Z	dimensionless
ℓ	finite difference time subscript	-
i	finite difference distance subscript	-
j	finite difference distance subscript	-
n_i	number of distance increments	-
n_ℓ	number of time increments	-
τ	infiltration opportunity time	T
$\Delta\tau$	infiltration opportunity time increment	T

Dimensions: **T** (time), **L** (distance)

Notation Used in This Report (cont.)

Notation	Description	Units
	Infiltration Models (Section E.2)	
Z	continuous flow cumulative infiltrated volume per unit length of furrow	L^3/L
Z'	surge flow cumulative infiltrated volume per unit length of furrow	L^3/L
P	furrow wetted perimeter	L
k	empirical infiltration coefficient	$L^3/(L \cdot T^a \cdot L^b)$
a	empirical infiltration exponent	dimensionless
b	empirical infiltration exponent	dimensionless
t_{on}	duration of first surge flow ON period (rt_c)	T
t_c	surge flow cycle time	L
r	surge flow cycle ratio	dimensionless
n	surge flow period	-
a'	surge flow infiltration exponent	dimensionless
k'	surge flow infiltration coefficient	$L^3/(L \cdot T^a \cdot L^b)$
$\tilde{k}$	step function infiltration model coefficient	dimensionless
$\tilde{a}$	step function infiltration model exponent	$L^3/(L \cdot T^a)$
$\tilde{c}$	step function infiltration model coefficient	$L^3/(L \cdot T)$
	Design Methods (Section E.3)	
L	field length	L
d	desired application depth at tail-end of furrow	L
Q_{in}	flow rate at the inlet to the furrow	L^3
n	Manning's roughness coefficient	$T/L^{1/3}$
S_b	furrow bed slope	dimensionless
k	empirical infiltration coefficient	$L^3/(L \cdot T^a \cdot L^b)$
a	empirical infiltration exponent	dimensionless
b	empirical infiltration exponent	dimensionless
t_c	surge flow cycle time	L
r	surge flow cycle ratio	dimensionless
μ_1	empirical furrow shape coefficient	L/L^{μ_2}
μ_2	empirical furrow shape coefficient	dimensionless
t_i	maximum time of irrigation	T
	Field Infiltration Tests (Section E.4)	
S_r	volume of water stored in infiltrometer resevoir	L^3
S_i	volume of surface storage in test section	L^3
c	constant of proportionality	L or L^2
$S_{drain,i}$	drainable storage in furrow test section	L^3
$S_{dep,i}$	depression storage in furrow test section	L^3
$\Delta Z_{adv,i}$	volume of infiltration during advance phase of test	L^3
$\Delta Z_{res,i}$	volume of infiltration during recession phase of test	L^3
ΔZ_i	increment volume of infiltration during i^{th} surge	L^3
ΔZ_i^*	measured volume of infiltration	L^3
Z_n	cumulative volume of infiltration	L^3
S_o	volume of surface storage in furrow (i=0)	L^3
τ	infiltration opportunity time	T

Dimensions: T (time), L (distance)

Notation Used in This Report (cont.)

Notation	Description	Units
	Principle Findings (Section F)	
obs	observed or measured value	-
pred	predicted or calculated value	-
r^2	correlation coefficient	dimensionless
t_c	surge flow cycle time	T
r	surge flow cycle ratio	dimensionless
k	empirical infiltration coefficient	$L^3/(L \cdot T^a \cdot L^b)$
a	empirical infiltration coefficient	dimensionless
b	empirical infiltration coefficient	dimensionless
$\bar{k}$	step function infiltration model coefficient	dimensionless
$\bar{a}$	step function infiltration model exponent	$L^3/(L \cdot T^a)$
$\bar{c}$	step function infiltration model coefficient	$L^3/(L \cdot T)$
Z	cumulative infiltration per length of furrow	L^3/L
P	furrow wetted perimeter	L
B	top width of water surface in furrow	L
h_o	maximum depth of flow in a parabolic shaped furrow	L

Dimensions: T (time), L (distance)